

Universidade Federal de Minas Gerais
Engenharia de Controle e Automação
NHL Stenden University of Applied Sciences
Lectoraat Watertechnology

Spark Detection And Prevention Device For Electrohydrodynamic Atomization Applications

Bachelor Thesis

Submitted by:
Mônica Emediato Mendes de Oliveira

Supervisors:
Prof. Luewton Agostinho, Dr., Prof. Klaus Glanzer, Dr.

Leeuwarden, 2022

Bachelor Thesis

Spark Detection And Prevention Device For Electrohydrodynamic Atomization Applications

Document submitted to the examining board designated by the *Lectoraat Watertechnology* at the NHL Stenden University of Applied Sciences and the *Colegiado de Engenharia de Controle e Automação* at the Universidade Federal de Minas Gerais as part of the requirements for approval in the subject Final Course Project.

Leeuwarden, 2022

Abstract

Electrohydrodynamic Atomization (EHDA), also known as Electrospray (ES), is a technology that uses a strong electric field (kV/cm) to manipulate liquid breakup into droplets. This technique allows the generation of droplets smaller than the nozzle diameter with a controlled droplet size, which means it can be used to produce uniformly sized particles in the micro/nanoscale range. This liquid spraying technique can generate different modes when both the liquid flow rate and the voltage vary with a narrow size dispersion. The most known mode is the cone-jet mode, because it can produce droplets in the micro- and nanometric range with a narrow size dispersion. Many authors [4, 10, 7] have published about the relationship between voltage, flow rate and droplet size for this mode. More recently, Verdoold et al. (2014) proposed the use of different variables based on current shape which can be used for classifying the ES modes.

In this work, the authors have developed an automated ES system called SmartSpark to relate the behaviour of the electric current for different spray-modes as well as during spark events, but also extracting values of the signal. We present a new approach which the focus is to provide an electric current data acquisition and signal processing tool that is capable to classify current shapes according to different electrospray modes, including the multi-jet mode and corona streamer onset regions. We present a new approach for the classification of the electrospray modes. The development of a Python library allowed completely automatic operation of the system, including setting of the electric potential and the liquid flow rate. After that, an electric current data logger was built with Raspberry Pi 4B+ and GSM HAT for Raspberry Pi so that we can have control and monitoring integrated with the SmartSpark.

Contents

1 Introduction	4
1.1 Motivation	5
1.2 Goals of the Project	5
1.3 Project Development Cycle	6
1.4 Electrospray Technique	7
1.4.1 Scaling laws	7
1.4.2 Electrospray Modes	8
1.4.3 Classification of Spray-modes	10
1.4.4 Streamer Corona and Transient Spark Discharges in air	12
1.5 Document Structure	12
2 Equipment, Experimental Setup and Method	14
2.1 Materials	14
2.2 Experimental Setup	15
2.2.1 Different Setups	18
2.2.2 Getting a Clean signal	19
2.3 Variables for the Measurement System	21
2.4 Validation	22
2.5 Uncertainties of the Instrument	23
2.6 First Electrospray Protocol	24
2.7 Project Activities	25
2.8 Design	25
2.9 Current Measurement	26
2.10 Protocol Measurement	28
2.11 Flow of Information in the SmartSpark	29
2.12 Data Processing	30
2.13 Statistical Analysis	30
2.14 Digital Signal Analysis	32
2.15 Viewer	34

2.16 SmartSpark Development	36
2.17 SmartSpark System Protocol	36
2.18 GasUnie B.V. Implementation Networks	38
2.18.1 InfluxDB and Grafana	41
2.18.2 Global System for Mobile Communication (GSM)	43
2.18.3 Raspberry Pi networked with GSM	45
2.18.4 Tunneling	47
2.19 Chapter Summary	50
3 Results and discussion	52
3.1 Electrospray Modes Classification	56
3.1.1 Non-automatic Control as First Approach	56
3.1.2 Automatic Approach	58
3.2 Spark Suppression	61
4 Conclusions	65
4.1 Recommendations	67
4.2 Proposals for Continuing, Limitations and Improvements	67
5 Appendices	71

1 Introduction

The history of electricity until electrohydrodynamic atomization can be traced back to the early days of man. Electricity was first discovered when man began to rub two pieces of amber together. This action created a static electric charge that could be used to power simple electrical devices. In the centuries that followed, electricity became increasingly important as it was harnessed to power increasingly complex machines.

In the late 18th century, Alessandro Volta developed the first electrical battery, known as the voltaic pile. This discovery led to the development of the first electric motors and generators. In 1831, Michael Faraday discovered that electricity could be used to create a magnetic field. This discovery led to the development of the electric motor. Faraday also discovered that electricity could be used to create light, and this led to the development of the electric light bulb. Faraday's work also laid the foundation for the development of the electric transformer. In 1876, Nikola Tesla developed the first alternating current (AC) electrical system. Tesla's AC system is the basis for the modern electrical power grid.

In parallel to this, the EHDA system was developed in the mid-1900s. This system uses electricity to spray a fine mist of charged droplets, which can be used to coat surfaces or to create a desired effect in a liquid. In the early 20th century, electricity was used to power the electrohydrodynamic atomizer. This invention allowed for the production of extremely fine droplets of liquid, which could be used in a variety of applications. Moreover, the use of electrohydrodynamic forces to disintegrate liquids from the micron down to the nanometer range in an orderly way, e.g. by so-called cone-jet electrospraying [31]; [26]; [30], has great relevance in the field of liquid atomization, with thousands of publications per year and commercial devices making use of it. Furthermore, since the droplets produced are highly charged, it has been applied with much success to the mass spectrometry of large biomolecules [10].

In the end of 20th century, the first publications [4] [10], [18] were concerned with the properties of the cone-jet, specially the electric current, because the current value is a direct indication of the type of energy expended and a parameter to predict droplet size. They did not look at the shape of the current signal. Later, the current signal study [28] published about the current signal, the shape of the current carries information about the spray-mode. This means that a general mapping between the properties of the current through the system and the spraying mode that is independent of the material properties of the liquid, the electrode geometry and other experimental conditions [28] allowed the present work to be written.

Therefore, in this work, we have carried an experimental study to address some of these questions in the context of classification of electrospray modes. The strong electric field (kV/cm) in the EHDA, generates the same pattern of spray-modes for different liquids. The present work will address a comparison with measurements done by other authors [4, 28]. In order to do this, a controlling and monitoring system of an ES has been implemented. We have aimed to 1) automate the system; 2) determine which spray-mode is operating in real time; 3) verify if appears any sparks; 4) data logger of the electric current.

For this, we have developed an automated ES system to relate the behaviour of the electric current for different spray-modes as well as during spark events, but also extracting values of the signal and data logging with a Raspberry Pi 4B+. The focus is to provide an electric current data acquisition and signal processing tool that is capable to classify current shapes according different spray-modes and sparks.

1.1 Motivation

The question which motivates this project is whether the EHDA setup could be fully automated. In an automated setup we could avoid discharges because power supply and all peripherals will be controllable. Avoiding electrical discharges is crucial for the stability of the spray and to guarantee it operates at the correct current level. Thus, even when spark risks are not foreseen, such device can/should be used.

Additionally, the development of the proposed device as the object of this project is extremely relevant for the continuation of this technology, as it is structured to create the necessary safety barrier which will allow the technology to enter the market in real scale. It has to be added, nevertheless, that its applicability, when proven feasible, can be extended to any application which involves the use of EHDA.

There are some advantages of ES technique over other atomization techniques: 1) Adjustable, narrow and constant size distribution; 2) Small particles; 3) Small amount of sample needed; 4) The aggregation is prevented since the charged droplets repel each other and therefore the size distribution is not distorted [20]. EHDA can be used at positive and negative voltage (DC), depending on the application requirements, or in alternating current. The potential applications for electric atomization are virtually limitless.

1.2 Goals of the Project

Initially, two demands were seen as crucial to improve the application of EHDA in industrial processes: 1) discharge prevention mechanisms and 2) non-visual monitoring and classification of the spray-modes. Both can be tackled via an automated system. The study of the behaviour of the electric current is done in an EHDA setup for different spray-modes as well as during spark events.

In order to verify a spark in an EHDA system, we need to get closer to a fully automated control of the spraying process. Hence, identify the current state of the spraying process, and, if necessary, adapt the voltage to obtain a stable electrospray mode. Furthermore, it also increases safety, hence recognizing sparks and in consequence reducing the supplying voltage automatically.

In parallel, there is a comparison with measurements done by other authors (validation) and a complete new and automated system that will collect and classify the data structures from the WiFi Oscilloscope (TiePie Engineering). The work has been done through software development using data structures (JSON) and the results presented were conducted through Python programming to communicate with the power supply (USB), pump (RJ11) and oscilloscope (WiFi) to classify the data collected of the system. For this, it was important as well to check the influence of the flow rate, electrical current, liquid properties (electrical conductivity, surface tension, viscosity, density), work distance, size of the nozzle, size of the syringe and generated mode. In addition, there is a monitoring system to verify if the electric current is on the desired spray-mode, done via Raspberry Pi 4B+ and a Global System for Mobile Communication (GSM) module.

In order to understand the electric current signal in the ES, it was necessary to automate the data collection system, as well as serial communication involving the setup's peripherals. Furthermore, we need the electrical current and voltage liquid. Real time analysis to verify the peaks, distribution and frequency of the current is also relevant on these scenarios.

We need to consider mainly the liquid flow rate and electric current signal, which will be important for the non-visual measurements as well as to control the entire system. We could obtain non-visual classification for each voltage applied in the setup. The literature addresses the linearity between

flow rate and the electric current [4] and reports about the characteristics of the ES electric current signal [28].

1.3 Project Development Cycle

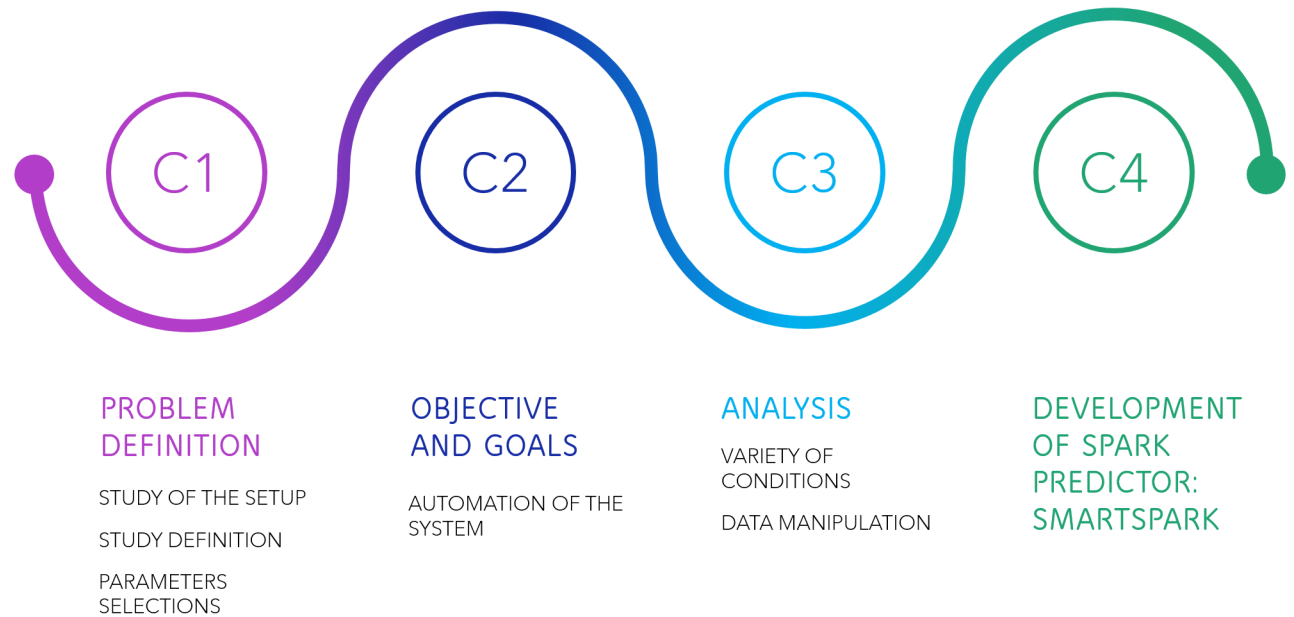


Figure 1. Development Cycle Method

The project development cycle followed the methodology shown in the figure 1. In this work, we have studied the behaviour of the electric current in an EHDA setup for different spray-modes as well as during spark events. In order to achieve that, we have automated the EHDA setup based on the study shown in section 1.4 in page 7. Afterwards, we have selected parameters that will be described later and then, we have conducted analysis of the data to achieve the goals of the project. From this, we have developed the spark predictor.

In relation to the innovation of this project, there are: (1) continuously measuring current and voltages in high voltage/low current applications with sample rates high enough (estimated 1 – 10 MS/s) to record all relevant signals (2) applying state of the art digital signal processing techniques to extract relevant current patterns to predict the onset of discharges, (3) integrate those technologies for a pilot setup, (4) develop a system (SmartSpark) to manipulate charges at the HV electrodes.

To do this innovations, this project is structured to investigate discharges under various conditions, i.e. different electrode formats/shapes, liquids, flow rates, surrounding atmospheres and temperatures. Such approach will help to create enough background to allow a generalization of the spark episode, i.e. a better understanding about the relation between the occurrence and the different setups used in EHDA and other external factors. Additionally, it will also focus on the circuit's manipulation after the detection, preventing a discharge and monitoring a high voltage system with sparks.

1.4 Electrospray Technique

A literature review will be presented about the technique used to solve the electrical discharge problem. Usually, the electrohydrodynamic technique involves forcing the liquid through a capillary and electrified needle. The electric field that generates the charged liquid can be used to power electric devices or to power other devices.

In an electrospray technique, a feeding liquid is pulled through a small orifice by means of an applied voltage. The resulting spray is electrically charged, and the droplets repel one another. The droplets are then accelerated towards the grounded electrode by the electric field. The size and shape of the droplets produced by the electrostatic atomization process depends on many variables that will be further explained, but our work is focus on the shape of the signal generated by the droplets because the automation of the system is based on it. The size of the droplets does not affect our system because the spray-mode will be reached anyway.

The behaviour of an ES system depends on many factors like the geometry, polarity, material properties, occurring discharges, etc. which is reflected in the measured currents. As a result, it can be rather different [28].

1.4.1 Scaling laws

For a certain range of values of both the applied voltage and the injected liquid flow rate, the electrified meniscus adopts an almost conical shape [19]. From the point of view of applications, the mode of greatest interest thus far has been the cone-jet mode in which the electrified meniscus adopts a conical shape, emitting a steady microscopic jet which leads to uniformly sized droplets [14]. The scaling laws are available for electrospraying in the cone-jet mode of polar liquids. Due to the fact that ES applications are continuously being developed, research on the underlying mechanisms will likely provide helpful insights for making this complex system reliable and robust in practical production settings. The electric spray current is a very important and explored variable in ES. It has been investigated by different authors [19], [10], [4], [18], resulting in scaling laws for the cone-jet mode, expressing the relationship between liquid flow rate, conductivity (two parameters that easily can be adjusted), surface tension, density and droplet diameter. Then, the scaling laws are useful tools for electrospraying practitioners since they can predict the order of magnitude of the size and charge of the emitted droplets [17].

Scaling laws are needed to characterize a defined ES system, providing better understanding of the mechanisms involved in the process [4]. Two different approaches have been used to obtain the scaling laws in the studies of [10] and [7].

The first author [10] published the following equations 1 and 2.

$$Q_o = \frac{\mu \cdot \epsilon_0}{\rho \cdot \kappa} [m^3/s] \quad (1)$$

$$I = \frac{\gamma \cdot \epsilon_0}{\rho \cdot \kappa} [nA] \quad (2)$$

Some parameters are: K = liquid electrical conductivity; Q = feed flow rate; I = current emitted; γ = surface tension; ρ = density; κ = dielectric constant; ϵ_0 = vacuum permittivity. For the second one [7] we have the following equations 3 and 4:

$$Q_o = \frac{\gamma \cdot \kappa \cdot \epsilon_0}{\rho \cdot K} [m^3/s] \quad (3)$$

$$I = \left(\frac{\gamma \cdot K \cdot Q}{\kappa} \right)^{1/2} [nA] \quad (4)$$

From the work of Chen and Pui et al. (1997) [4], we have a proportionality function based on the previous studies that can be seen in 5.

$$\alpha = \left(\frac{K \cdot Q \cdot \gamma}{\kappa} \right)^{1/2} \quad (5)$$

1.4.2 Electrospray Modes

It was found that for Electrospraying modes resulting in a pulsed current, the pulse shape differs significantly between different spraying modes and various stages in the development of a pulse were identified [28]. There are four common modes of EHDA: dripping, intermittent, cone-jet and multi-jet. There is an electrical current difference between EHDA modes. In the ES context, dripping mode occurs when the liquid being sprayed is broken up into small droplets due to the electrical potential applied to it. The liquid droplets are then driven towards the electrode and are eventually deposited onto the surface (Figure 2 A and 2 B).

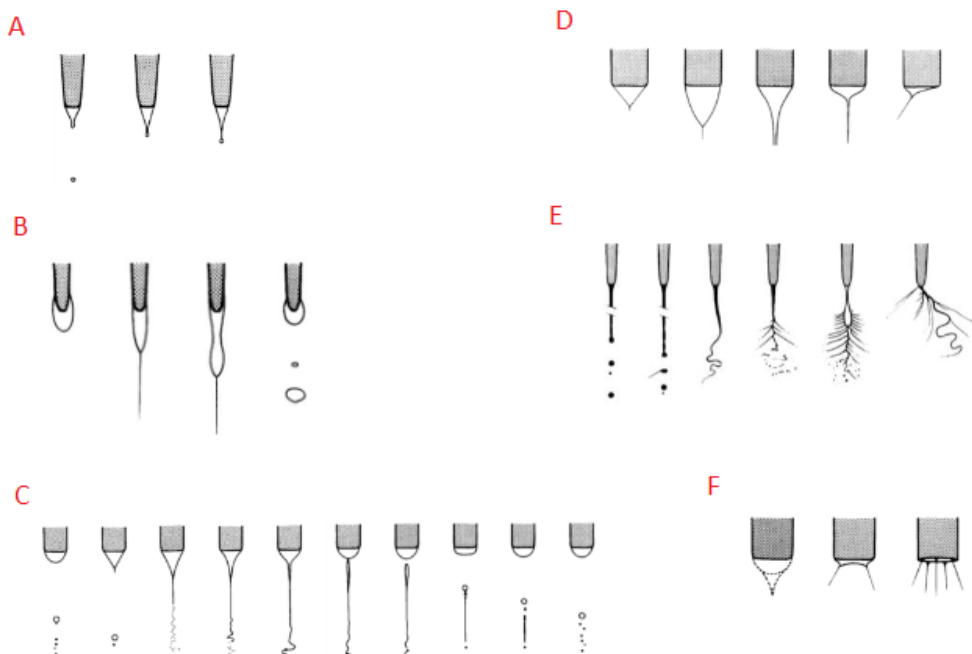


Figure 2. Spray-modes [19]

Intermittent mode is when the spray is turned on and off at regular intervals. This can be used to control the amount of liquid that is sprayed, and can also help to prevent clogging (in the Figure 2 C and 2 E). Cone-jet mode is a type of ES in which a cone-shaped spray is produced, with the droplets at the apex of the cone being the smallest. The cone-jet presents some different characteristics according to the literature and has some differentiations as can be seen in 2 D in the Figure 2.

Taylor [26] was the first to demonstrate that electrostatic pressure and capillary pressure can be balanced at any point on the surface of a liquid cone. The creation of a permanent jet, for its part, requires a penetration of the field lines in the liquid, so that the liquid must not be a perfect conductor. For liquids with relatively high conductivity, the jet formation zone is limited to the apex of the meniscus [30]. Therefore, we shall use the term "cone-jet", whether the meniscus has a form corresponding essentially to a "Taylor cone" or to a "convergent jet" [19].

We consider the cone-jet configuration of figure 3. The steady Taylor cone-jets naturally occurs under relatively limited circumstances: when the applied field and flow rate are in the appropriate range, and the electrosprayed liquid exhibits the adequate physical properties, which entails having a field profile along the liquid surface necessary to get a potential drop in the liquid, from the polarizing electrode (either an immersed one, or the conductive capillary itself) to the cone apex, to accelerate the converging interfacial liquid to form the jet. This phenomenon exhibits certain physical balances and delicate symmetries which have attracted the attention of many researchers over the last decades, although still fundamental questions about the mechanisms responsible for both the establishment of steady Taylor cone-jets and their stability remain unanswered [17].

Additionally, there exist some variations within the cone-jet mode. There is the varicose breakup, where the drops are round at the end of the jet. In the cone-jet kink instabilities we have whipping breakup (see Figure 5b IV and Figure 5b V). This work does not differentiate this on the classification.

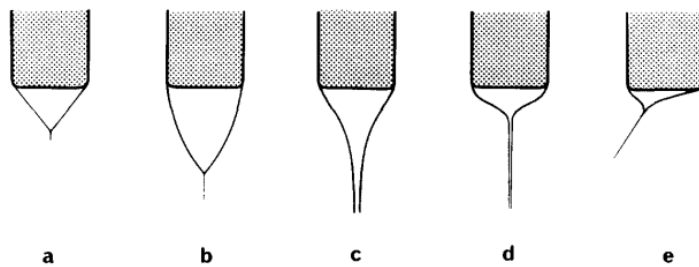


Figure 3. cone-jet modes [19]

During the cone-jet, multiple parameters and variables influence the current, flow rate and voltage operational window (see Figure 4). The operational window can be defined where the ES cone-jet mode can be stabilized based on the flow rate, voltage and the setup configuration [11]. To explain the Figure 4 of the voltage window, the first and last point on the X axis is the minimum and maximum flow rate respectively. Between the minimum flow rate and the upper final point we have the voltage window on the Y axis. The window formed by these points is where the system operated in the stable cone-jet. Operational windows depend of the liquid and configuration setup.

In the X axis from the Figure 4 there are equations 6 until 8.

$$Q_o = \frac{\epsilon_o \cdot \mu}{\rho \cdot K} \quad (6)$$

$$Q_{min} \propto Q_o \quad (7)$$

$$Q_{min} = const \cdot Q_o \quad (8)$$

In the Y axis from the Figure 4 there is the equation 9.

$$\gamma_I = \frac{\mu}{\rho \cdot K} \quad (9)$$

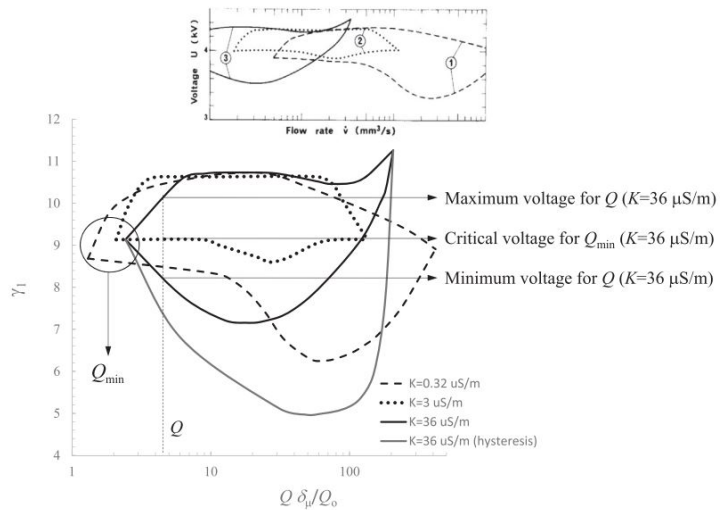


Figure 4. Operational window for cone-jet mode [17]

There are many model theories concerning these equations 8 and 9, however, one can generalize that the minimum flow rate guarantees that the experiments are at a meeting where we will have a constant jet. A group of symmetries rising at the cone-to-jet geometrical transition determines the scaling for the minimum flow rate and related variables. If the flow rate is decreased below that minimum value, these symmetries break down, which leads to dripping [12].

Finally, the multi-jet mode is a mode of operation in which multiple streams of liquid are emitted from the nozzle (see letter E and F in Figure 2). This mode is typically used when a high flow rate is required, or when the liquid being sprayed is viscous.

1.4.3 Classification of Spray-modes

In Verdoold et al. (2014), spray-mode types are summarized, their relationship to current shapes are demonstrated and classified based on statistics proposed (see Figure 5a and 5b). The spray-modes are distinguishable by the current shape or level. "For signals containing strong discharges and/or significant fluctuations the smoothing approach may not be sufficient. Using higher sampling rates may help in those situations" [28]. To describe the complete signal, all pulses need to be located individually. And after this, the results of all individual pulses are used to describe the complete signal. Classifying spray-modes from electric current signal shapes would allow non-visual identification in opposite to visual classification.

In Figs. 5a and 5b we have configurations 10, 12 and 15. gener

- Configuration 10: type I is the nozzle-to-plate configuration; the needle type has the outer diameter (OD) of the capillary (d_{cap}) = 0.71 mm; the inner diameter (ID) of a capillary ((d_{cap}),in) = 0.41 mm; distance from capillary and the plate (Lp) = 30 mm; resistance = $1 \times 10^6 \Omega$ [27].
- Configuration 12 type I is: the nozzle-to-plate configuration; the needle type has the OD of the capillary ((d_{cap})) = 0.91 mm; the ID of a capillary ((d_{cap}),in) = 0.61 mm; distance from capillary and the plate (Lp) = 30 mm; resistance = 9760Ω [27].
- Configuration 15 type IV is: the nozzle with ring and plate configuration; the needle type has the OD of the capillary ((d_{cap})) = 2.00 mm; the ID of a capillary ((d_{cap}),in) = 0.20 mm;

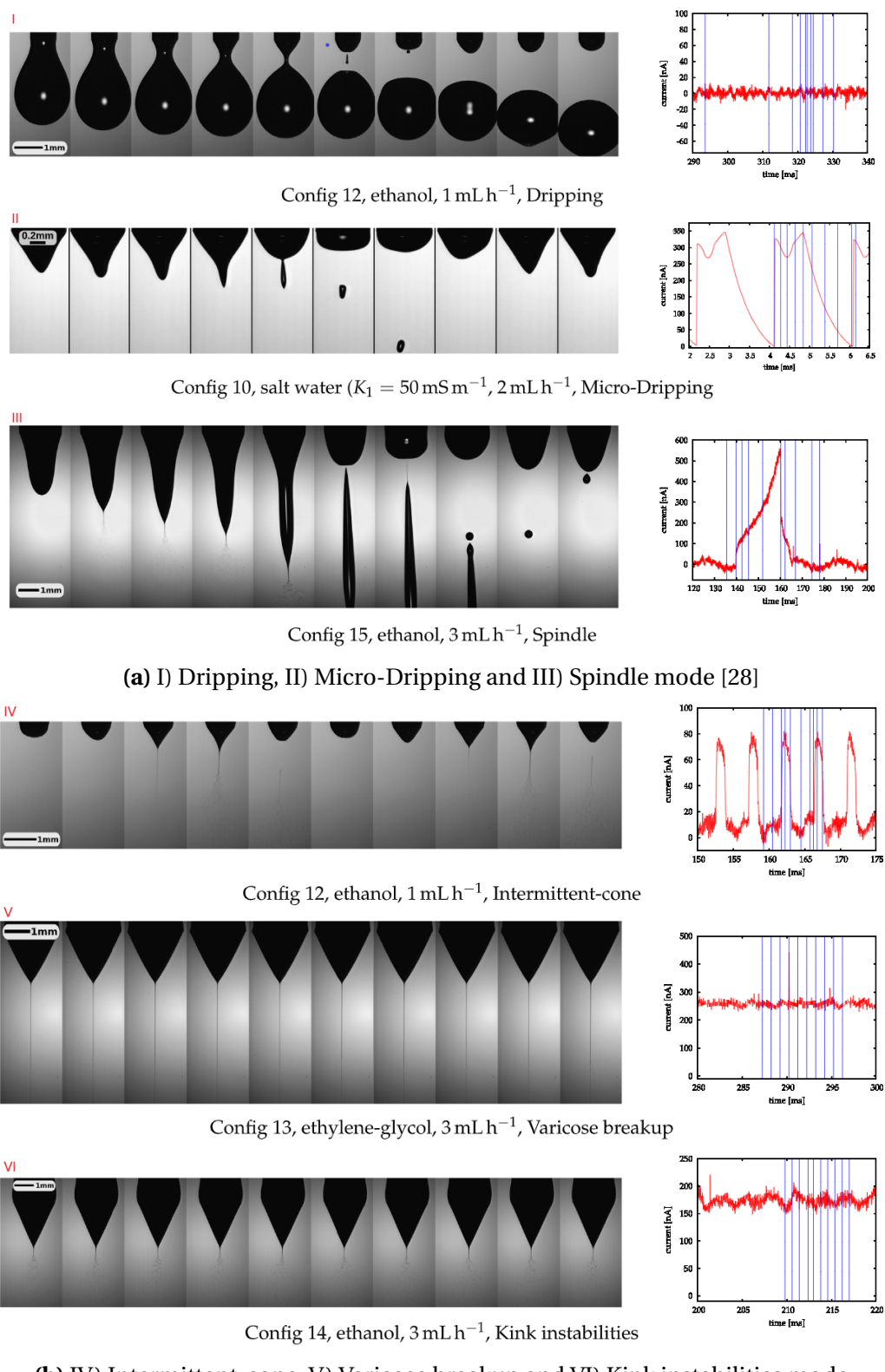


Figure 5. Liquid menisci and electrospray current signal for different spraying modes. The moments the images were taken are indicated by the added vertical lines in the current characteristics [28]

diameter of the ring (dring) = 20 mm; distance from capillary and the plate (Lp) = 70 mm; resistance = 9760 Ω [27].

Control variables are implemented for three spray-modes (dripping, intermittent, cone-jet) [28]. Grounded plate and charged (HV) nozzle, nozzle diameter, nozzle-to-plate distance, flow rate and setup were defined according to this papers. Verdoold et al. (2014) had done classification related to the shape of each current. They addressed different variables for each mode of the ES. It was possible to see their classification on the measurements conducted in the High Voltage Lab.

Interestingly, the present work are extending the non-visual classification method initiated by the author Verdoold et al. (2014) using modern acquisition and signal treatment methods and adding new approaches for it. We also have integrated the signal in real time and in a data logger.

1.4.4 Streamer Corona and Transient Spark Discharges in air

At atmospheric pressure, glow discharges in air easily transition into spark discharges that significantly heat the gas, which is problematic for applications sensitive to temperature [23]. Two types of DC discharges of both polarities operating in atmospheric air with/without water were applied: streamer corona (SC) and transient spark (TS) [1]. Their electrical parameters and emission spectra are different and this is not relevant for the present work. The difference between SC and TS can be seen in Figs. 6 and 7 from different authors.

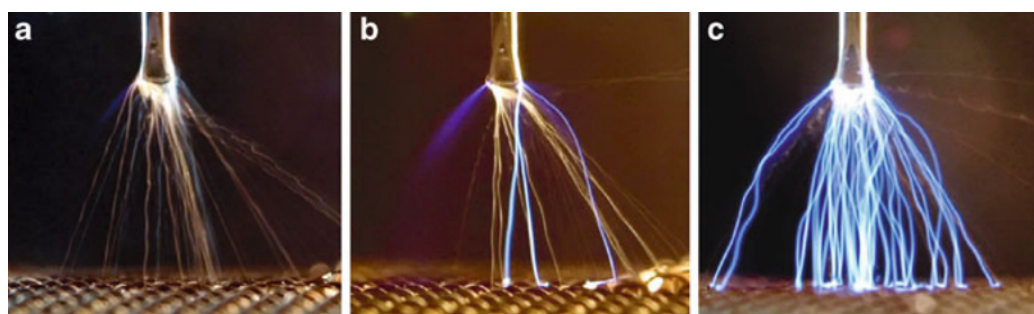


Figure 6. Photographs of the ES of water in 8 mm gap, water flow rate 0.5 mL/min, exposure time 1/10 s: A) ES with SC, 6.5 kV, B) transition SC-TS, 7.8 kV, C) TS, 9 kV [1]

SC transient bandwidth needs to be measured, if the voltage is increased to a level that is usually beyond the need of normal operational window for ES, corona develops at the nozzle. This depends on the shape of the nozzle, humidity, atmosphere composition (natural or artificial), distance to collector plate. The corona is a prerequisite for partial discharges and full discharges.

The analysis of sparks requires a relation between liquid properties, flow rate, electric current and electric voltage that will be described. In stable ES system, currents are usually between 10 and 300 nA. On the other hand, with corona occurring at the nozzle currents go up to a few μA. Corona noise could be classified because of the frequency, which classify the signal. The distance between two signals can be shifted but the characteristic filters is in the signal.

1.5 Document Structure

The structure of the thesis will be based on the methodology shown in the figure 1, the document will follow these steps. Based on the technique description, we could select the parameters to succeed the goals in this chapter, select the validation of the system based on published papers.

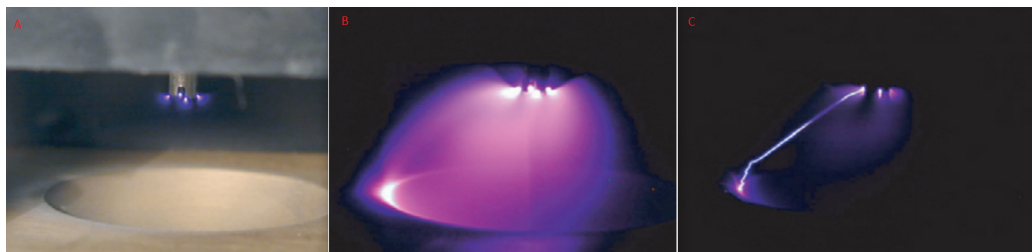


Figure 7. View of pin-to-plane discharge in ambient air in different current regimes. The inter-electrode gap is 15 mm. A) True negative corona in air, $I \leq 200 \mu\text{A}$ (B) DC steady-state diffusive glow discharge in airflow, $0.3 \leq I \leq 3 \text{ mA}$. (C) Transient spark in ambient air, $I \leq 0.3\text{--}1.3 \text{ A}$ [3].

Furthermore, knowing how the research on the EHDA topic was done is important, as well as knowing how to classify the spray-modes. Several works aimed at classifying ES modes have already been published.

In the further chapter, the methodology will be described. The setup configuration, security aspects, cabling, how is the data management system and the instrumentation were explained. In addition, there will be information about details about the automatic setup, Python library implementation, data logger development, classification criteria and future outlook regarding the automation system.

At last, we present the results with the development part explained and where most of the software development was done in order to automate the EHDA setup. In parallel to this, an analysis based on a variety of conditions experiments and data preparation and manipulation was made. We found out which conditions are important and which variables were chosen to the automation of the process in this cycle.

After that, we discuss the results and suggest further steps for future and suggestions for the future. Additionally, the conclusions will be presented with some remarks and proposals for continuity.

2 Equipment, Experimental Setup and Method

In this chapter, we describe the process and formulate the problem. Since this is a document in control and automation engineering, it is essential to present materials, setup, instruments, process sensors, actuators and practical development.

Firstly, we will give the first step further in the automation process. Our goal is to gain better knowledge about the variables of the process, as well as the configuration procedures. There are information about materials, experimental system, configuration, electrical discharges, current measurements, measurement process, safety aspects and getting a clean signal.

Secondly, the method used was based primarily on the publications already made related to the EHDA technology. For this, we have performed the measurement protocol, design, system activities and requirements. This chapter covers this and the development necessary to built the project.

Furthermore, details about different setups, the data processing and the signal processing analysis and the closed loop system will be explained. After that, there is the information about how to use the SmartSpark system.

2.1 Materials

The materials of the setup consist of one power supply (brand: FUG, model: HCP35-20kV) and a pump (brand: master dual, model: WPI AL-1000) that can both be controlled via USB serial connections. The power supply's (HVPS) internal voltage and current measurements can be polled via an USB interface and it is included in the data logging.

HVPS provides the electrical potential to the liquid, which can be applied by connecting the HVPS directly to the liquid feeding capillary or needle to a grounded electrode (usually a plate or a ring) located downstream. The setup has the USB interface for controlling and polling measurements. To do the USB serial connection with the HVPS we have used the USB Cable 2-in1 Type C. The configuration was made on a Windows PC, following the manuals of its website and with the Baud rate of 115200.

The interface between the syringe pump and the computer, a DB9 to RJ11 cable was made. In order to do the connection between nozzle and Power Supply, we have used the mounting Instruction for Plug HS21 + Cable 130660.

Most of the current measurements were performed at the nozzle-to-plate configuration. The material used for the nozzles was made of conducting materials. Current flows in the high voltage line with banana plug connection.

The current is measured via a TiePie WifiScope WS6 from TiePie engineering that is a battery powered oscilloscope capable of transmitting data via a WiFi connection allowing it to be placed in the high voltage or ground path. The current is routed directly via the input, hence the oscilloscope measures the voltage dropped via its input resistance (which can be switched between 1 or 2 M Ω).

TiePie WifiScope WS6 has a resolution of up to 16 bit at a minimal input range of 200 mV, sufficient to measure currents down to 1 nA. One of its functionalities is that the measurement displayed is constantly updated during the experiment. The result do not have to wait until the whole measurement is completed to be shown. The signal analysis with an oscilloscope using WiFi technology allows an in-depth case study of the electric current signal.

Regarding the system environment control, we have the relative humidity. It is an important

Table 1. Liquid properties

Name	Supplier	Formula	Molecular Weight
Ethanol absolute (>99.7) 3	VWR Chemicals	H_3CCH_2OH	6.07 g/mol
2-Propanol (>99.9) HiPerSolv	VWR Chemicals	$(CH_3)_2CHOH$	60.1 g/mol
Ethylene Glycol	Fisher BioReagents	$C_2H_6O_2$	62.068 g/mol (20 °C)

parameter because it can affect the physical properties of the liquid and for this reason we included in the setup a Temperature and Humidity Sensor with 1-Wire bus. The DHT11, DHT22 (also called AM2302) are modules that measure temperature and humidity and transfer the digitized values over a 1-Wire bus. To use them with the Raspberry Pi, a 1-Wire driver written in C/C++ has to be used, because of the tight requirements for the timing using short pulses in the order of 10-100 μ s. At the moment two driver sources are available, one from Adafruit und one that is part of the pigpio library. The installation process for both packages is simple, but the pigpio version needs a daemon to be started before the user program runs. The "Adafruit-DHT-Fixed" library package was chosen to interface between instruments.

The capillary used was a PEEK Tubing 1/16" Outer Diameter (OD), 0.030" Inner Diameter (ID). The flow impedance of tubing/capillary is very important. The functions of the spray capillary are: 1) liquid transport from vessel to sprayer tip; 2) current transport from current coupling location to sprayer tip (via capillary material or liquid inside the capillary); 3) providing a contact geometry for the Taylor cone.

In relation to chemical experiments, solution preparation and characterization are important steps in order to ensure the validity of the results. The preparation of the solutions begins by following the basic safety information needed to perform the procedure. All the chemical reagents were used as purchased, without further purification. The liquids used in the experiments are presented in the table 1.

Finally, characterization of solutions includes measuring the surface tension (DCAT – Dynamic Contact Angle measuring devices and Tensiometer, Ring and plate tensiometer DCAT 9, by Data-Physics Instruments at WETSUS); Electrical conductivity (approach at Van Hal Larenstein with 912 Conductometer from Metrohm); Viscosity (measurement approach at WETSUS Rheometer Modular Compact Rheometer: MCR 102 from Anton Paar Instruments); and density. These measurements will be used in combination with the geometry of the setup in order to do the automation of the system.

To visually double validate the ES-mode classification there is a high speed camera imaging (Photron with a Navitar 125x microscopic lens). It runs in parallel to the experiment providing continuous monitoring of the ES modes.

2.2 Experimental Setup

In this work the authors designed a setup, using measurement instruments in combination with real-time signal processing to create a system which allows real-time classification of the electric current using WiFi Oscilloscope in EHDA system. Because we automated the system, this work includes spark detection and in consequence allows discharge suppression which is one of the goals for this funded project that was only available because of the automation of the process.

Since the goal is automate the system to detect and prevent nozzles to counter electrode discharges, we take the following approach: 1) continuously measuring the electric current with high sample

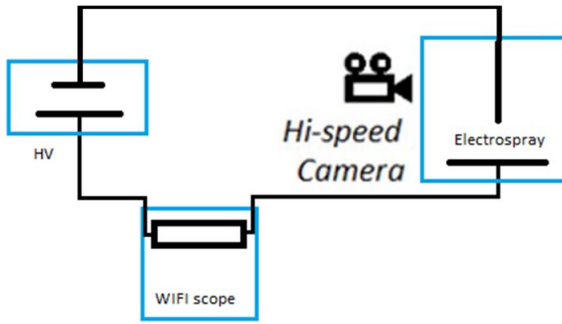


Figure 8. EHDA nozzle-to-plate circuit

rates; 2) real-time processing of the current signal; 3) real-time classification spray-modes and sparks discharges; 4) real-time recognition of sparks at nozzle; 5) recognize partial and full discharges in corona; 6) recognize ES mode via current measurement; 7) modulate voltage at nozzle; 8) data logging of the electrical current. The partial discharge can be described as the one that happen inside the ionized corona gas, or from the corona to the surrounding atmosphere. The full discharge is the nozzle to collector discharge/ARC. The electric circuit of the experimental system can be seen in Figure 8. It is highly recommended that we make a simple electric-mechanical schematic of the set-up as in the Figure 8 or 11.

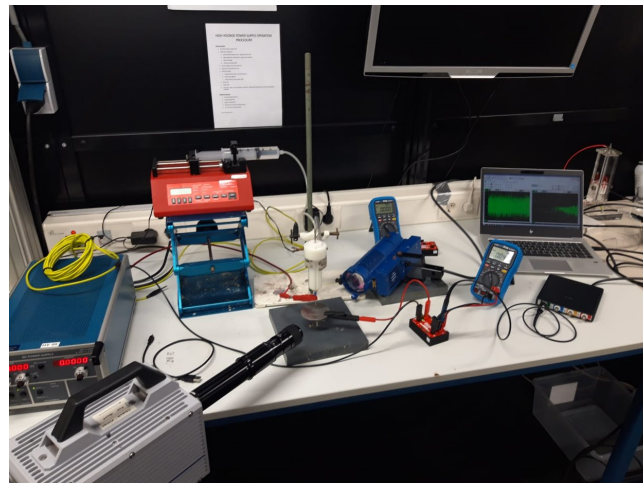
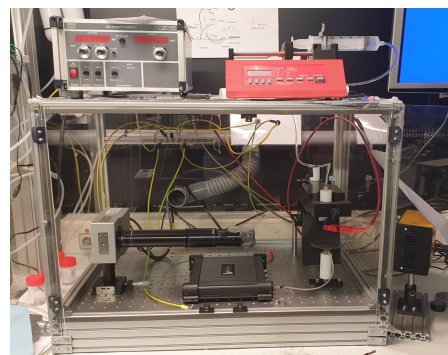


Figure 9. First setup

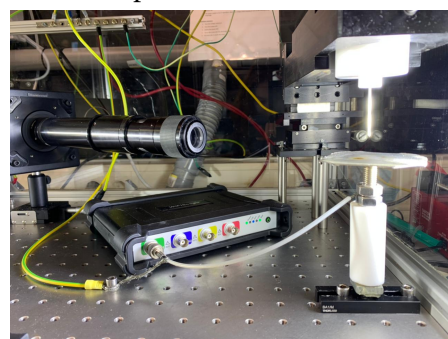
The first setup in the High Voltage Lab is in the figure 9. This picture was taken by the NHL Stenden Water Technology Group a couple years ago. The setup was built without the cabinetry that helps the environment to be constant and noise-free. In the left side you can see the Power Supply, the High Speed Camera, the pump connected to the needle via capillary, the nozzle support for the needle, the High voltage cable from the Power Supply to this nozzle and the Oscilloscope from TiePie connected to the PC via USB joined with the multimeter in the ground line.

The Experimental System of this work mostly use the EHDA nozzle-to-plate setup with cabinet 10b. Figure 11 shows the diagram of the setup explained. Meanwhile, we can see the the setup with the cabinetry implemented 10b and nozzle-to-plate configuration, where the high voltage is applied in the white nozzle. The diagram of this setup is similar as 11. The information about the nozzle will be in the following chapter.

The distance configuration, the work distance between nozzle and plate in a nozzle-to-plate configuration (see the Figure 10) and the properties of the liquid are important. Another variable is



(a) Optronis CR450x3 high speed: 1-6010 ; S/N 1835-SX-043 and 1x Adapter 1-6016 NAVITAR 12X



(b) New high speed camera and flash power one on the nozzle

Figure 10. Setup nozzle-to-plate (*EHDA nozzle-to-plate setup*)

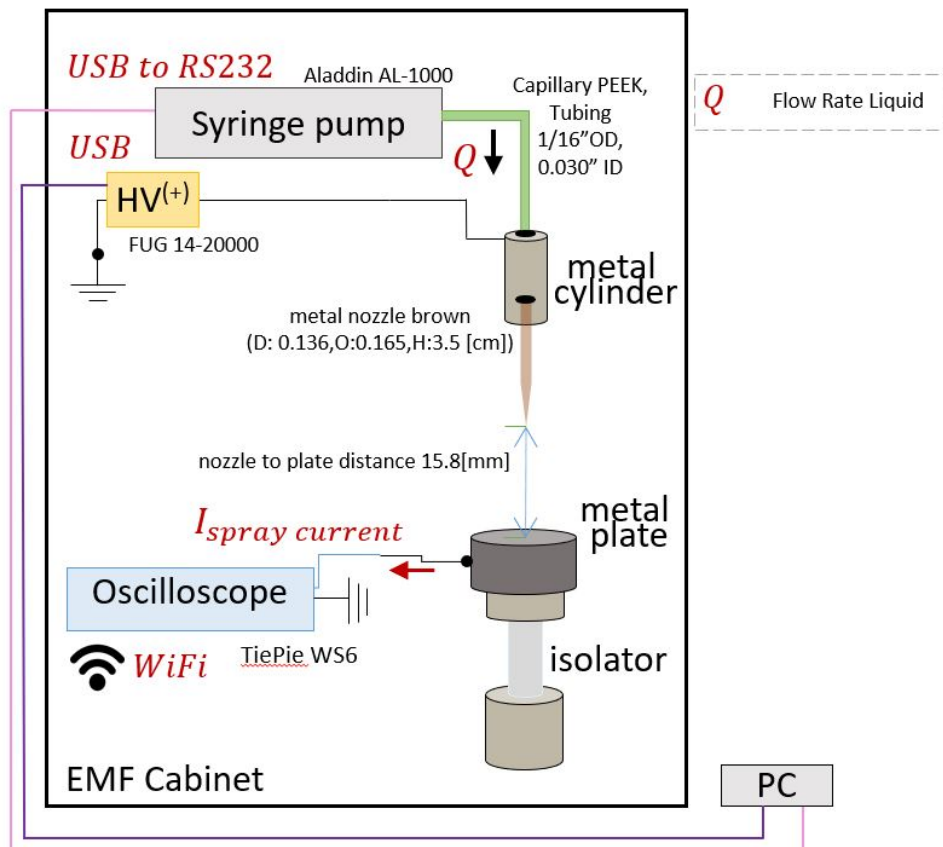


Figure 11. EHDA diagram setup nozzle-to-plate and ground line setup

the atmosphere (temperature and humidity), but it does not affect so much inside of an Electro Magnetic Field (EMF)/Radio-Frequency Interference (RFI)-shielded of 60 cm box, but in industrial cases it has to be analyse. Finally, everything is linked to the flow rate of the pump.

In relation to the flow rate, there should not be fluctuations in flow rate. The flow rate is independent of ambient pressure fluctuations and the pump can be simple and cheap. It is important that there is no dead volumes or cross-contamination.

It is likely desired that you have optical access to have a stable jet by high speed camera in the setup. It is good to know that for high speed images you need more light and distance. For low speed images you do not need a lot of light.

In relation to the liquid feed, the tool box is easily adjustable and the flow impedance of tubing/capillary is irrelevant. The experiments were conducted following the rules: 1) Liquid and electrolyte properties; 2) Physics and processes; 3) Available materials.

The setup has short term flow fluctuations and limited duration of continuous operation and there is a risk of damaging the syringe pump if the high voltage supply is applied directly to the capillary and dead volumes of the liquid. The ventilation system is installed in the setup in order to maintain the circulation of air and when working with toxic fluids like NHO₃, n-Heptane, N-Dimethylformamide is important.

The setup is made with the data logger, the routine, control software for industries, file structure (which means unlimited data), real time classification, the setup design and required liquid properties must be adapted to the application. In the setup design, it is necessary to be aware of what is relevant for the application and make decisions.

2.2.1 Different Setups

Besides the nozzle-to-plate setup, other setup implementations were made for testing. Testing may be repeated, specifically to check for errors, bugs and interoperability. This testing was performed until the advisors find it acceptable.

For the GasUnie B.V. project (subchapter 2.18), it was not possible to access the plant ground line. Therefore, cabling had to be developed which integrated the HV on the nozzle side, i.e. current only at the HV. For this purpose an isolated cable box was developed. The oscilloscope was in series with the power supply and nozzle as you can see in the 12.

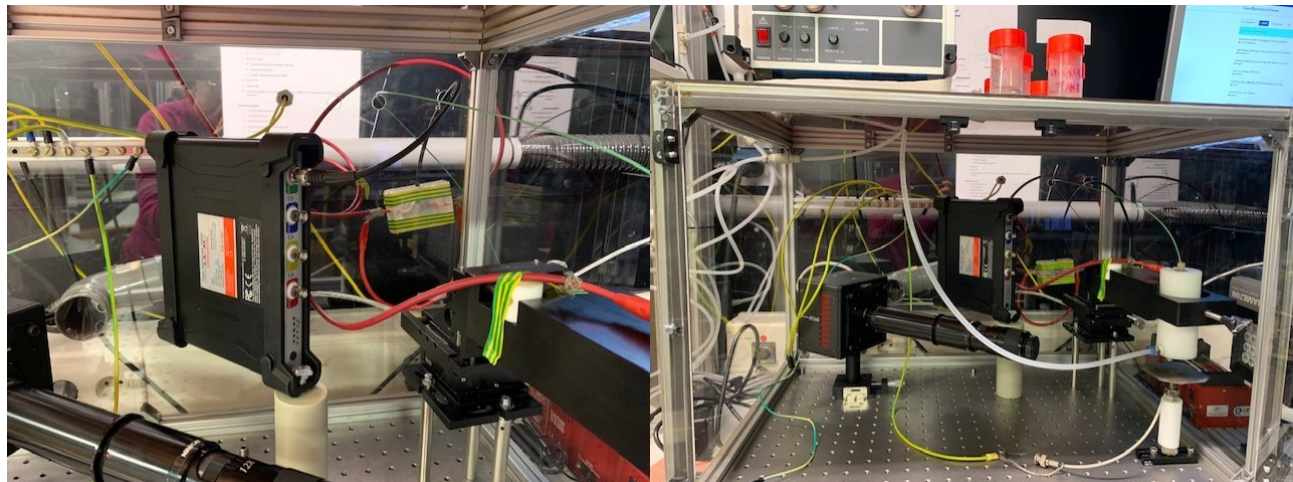


Figure 12. Oscilloscope high voltage side

In parallel to this, experiments with the ring in the nozzle were conducted. The diagram of setup can be seen in the figure 13.

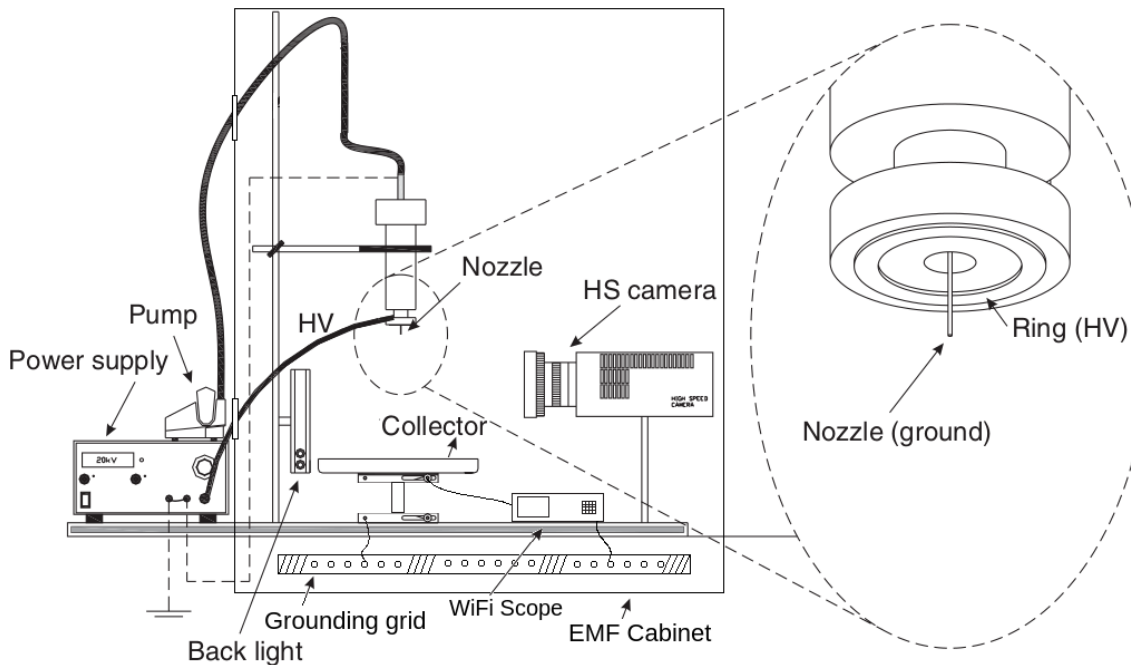


Figure 13. EHDA diagram setup with ring (*EHDA ring setup*)

Furthermore, we have implemented the co-flow. The co-flow implementation had some reasons as: 1) to keep the relative loads of the atmospheres constant; 2) to further stabilize the cone-jet; 3) to decrease the differences in measurements from one day to the next. This system was implemented as the Figure 14 is displayed.

Finally, it is possible that there are variations in the process so there is monitoring of the system on the ground and high voltage line in real time for double validation. To do this we have developed the setup in the figure 15.

2.2.2 Getting a Clean signal

The major causes of noise in high voltage connections are electrical interference, mechanical vibrations, and thermal noise. Electrical interference can come from external sources such as power lines, electrical appliances, and lightning. Mechanical vibrations can be caused by moving parts in the system, such as fans or pumps. Thermal noise is caused by the random movement of electrons in the system.

Inductors and conductors are both types of electrical components that are used to create and conduct electricity. Both can be found in a variety of electronic devices, but they serve different purposes. Conductors are typically made of metal, and they are used to carry an electrical current from one point to another. Inductors, on the other hand, are typically made of a coil of wire and are used to store energy in the form of a magnetic field.

When electricity flows through a conductor, it creates a small amount of noise. This is because the current flowing through the conductor creates a magnetic field that interacts with the electrons in the conductor. This interaction causes the electrons to vibrate, which produces a small amount of noise. Inductors also produce a small amount of noise when electricity flows through them, but this noise is caused by the changing magnetic field that is created by the inductor.



Figure 14. Co-flow system

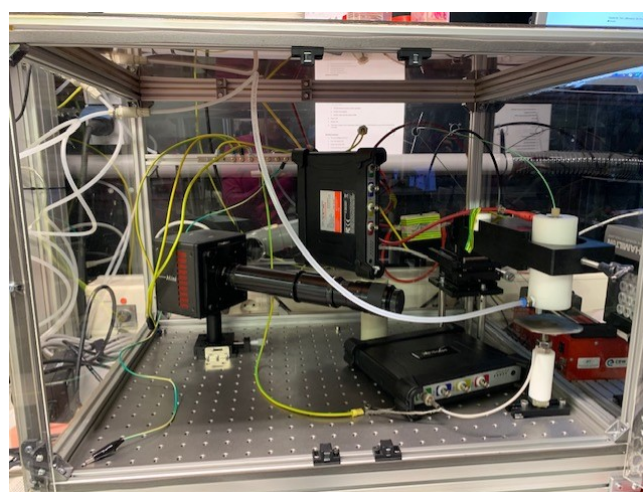


Figure 15. Oscilloscope high voltage and ground side

The first step was based on avoiding 50 Hz coupling. There are a few ways to avoid 50 Hz coupling:

- 1) Use a Faraday cage: This is a cage made of conductive material that surrounds the circuit and prevents 50 Hz coupling.
- 2) Use a transformer: This device transforms the 50 Hz coupling into a different form that is not harmful to the circuit.
- 3) Use capacitors: These devices block the 50 Hz coupling from reaching the circuit.
- 4) There are usually 3 phases 220/400 V system: connect noisy power adapters (switch mode power adapters) to another phase than the oscilloscope and HV power supply.
- 5) Star grounding (in a single point).

The second step was keeping general EMI (electromagnetic interference) low. This can be done via:

- 1) Route the high voltage supply cables and probe leads distant from power cables for e.g. HV-power supply, light source, pump, camera, etc.
- 2) Keep the oscilloscope probe cables as short as possible.
- 3) Keep cables pairs (feed and return currents) together.
- 4) Do not create loops with a large cross sections.
- 5) There are also some noise that could be reduced further by shielding some parts or simply rely on filtering at e.g. 15 kHz. The approach of rearranging power cables and connecting to devices to different 240V phases worked out and it reduced 50 Hz pickup and noise.

2.3 Variables for the Measurement System

Measurement is a set of operations that aims to determine a value of a quantity. Measurement instrument is a device used for a measurement, alone or in conjunction with more devices. Measurement system is a complete set of measurement instruments and other equipment coupled together to perform a specific measurement [8].

Measurements can be used in applications for monitoring and control. The first, monitoring, can be focused on signal processing, such as:

- 1) passive, non-acting observation;
- 2) identification of predominant behavior;
- 3) identification and mathematical modeling;
- 4) estimation of parameters or state [24].

During the ES process, multiple parameters and variables influence the current, flow rate and voltage. These parameters can be divided into geometric, liquid properties and controlled variables. The properties of the liquid have different effects on the ES system, this means that changing one parameter can affect the others which makes it difficult to isolate these properties.

As for the SmartSpark configuration variables, there is a division between setup and liquid properties. The setup has the geometric variables related to the type of nozzle, syringe and configuration that we have been using. The liquid properties are explained in numeric topics bellow.

0. Conductivity: the conductivity of the liquid determines the amount of charge that can be carried by the liquid flow, and hence the maximum charge that can be carried by a droplet. The higher the conductivity, the higher the maximum charge, and the smaller the droplets. The basic unit of measurement of conductivity is the mho or siemens. Conductivity is measured in micromhos per centimeter ($\mu\text{mhos}/\text{cm}$) or microsiemens per centimeter ($\mu\text{s}/\text{cm}$). Conductivity plays a big role in the behaviour of the ES measurements.

In general, the conductivity of the liquid has a strong effect on the size of the droplets, and hence on the performance of the ES system. The conductivity also affects the stability of the droplets, and can be used to control the size distribution of the droplets.

1. Density: The density of the solutions being sprayed is important to determine the minimum flow rate necessary to reach the cone-jet [24]. The SI unit for density is kilograms per meters cubed (kg/m^3).

2. Viscosity: This property represents the resistance a liquid has to flow. In an ES system, the liquid

is typically forced through a small orifice by a high-voltage electric field. The high electric field causes the liquid to break up into small droplets, and the viscous liquid flow ensures that these droplets are relatively uniform in size. The viscosity of the liquid is a function of the temperature and the pressure.

3. Surface tension: When an electric field is applied to a liquid, the liquid will be drawn to the electrode. This is because the molecules at the surface of the liquid are attracted to the electrode. This creates a tension at the surface of the liquid. The surface tension of the liquid is an important factor in determining the size of the droplets that are produced. If the surface tension is too high, the droplets will be too.

In an ES system, surface tension can affect the magnetic field around a body of liquid. If the surface tension is strong, it will tend to hold the magnetic field lines close to the surface of the liquid. This can make the magnetic field stronger near the surface of the liquid. If the surface tension is weak, the magnetic field lines will be able to penetrate further into the liquid and the magnetic field will be weaker near the surface.

We have separated the configuration in two: 1) setup: information about the setup; 2) liquid: properties of the measured liquid. The present work does not attempt to clarify the effects of other variables included in the ES process that were not measured, such as the dielectric constant.

2.4 Validation

The complexity of electrohydrodynamics is difficult to find in other fields of mesoscale physics. Even in simple situations, where the system adopts a steady or quasi-steady regime, the high dimension of the parameter space and the lack of precise experimental information have precluded a comprehensive and accurate description of the problem. The steady Taylor cone-jet mode of electrospraying constitutes a very good example of this [17].

Because of that, the system should be validated based on scientific papers in order to ensure that it is effective. This will help to ensure that the system is able to provide accurate results and that it is able to meet the needs of the users.

In order to do this, it is important to have a database with the data of the authors who have already published about their experiments. Initially, the validation is implemented for cone-jet because of the equation in 5. We have the same solutions as Chen and Pui et al. (1997) work [4].

In addition, we have the same liquids as several other authors and this was positive to verify that we are following the same path. To choose the liquids, the figure below 16 was analysed, as well as other papers [28] and [4] and with the liquids available at the Water Technology Center (WAC).

$$I/I_o = 2.6 \cdot \left(\frac{Q}{Q_o} \right)^{1/2} \quad (10)$$

$$Q_o = \frac{\sigma \cdot \epsilon_o}{\rho \cdot K} \quad (11)$$

This minimum flow rate indicated in the X axis from the Fig. 16 is explained in the Eq. 11 is from the liquid in the pump, what moves a fluid through a pipe or other system. It is caused by the fluid's pressure and is perpendicular to the direction of flow. In the Y axis we have the Equation 10.

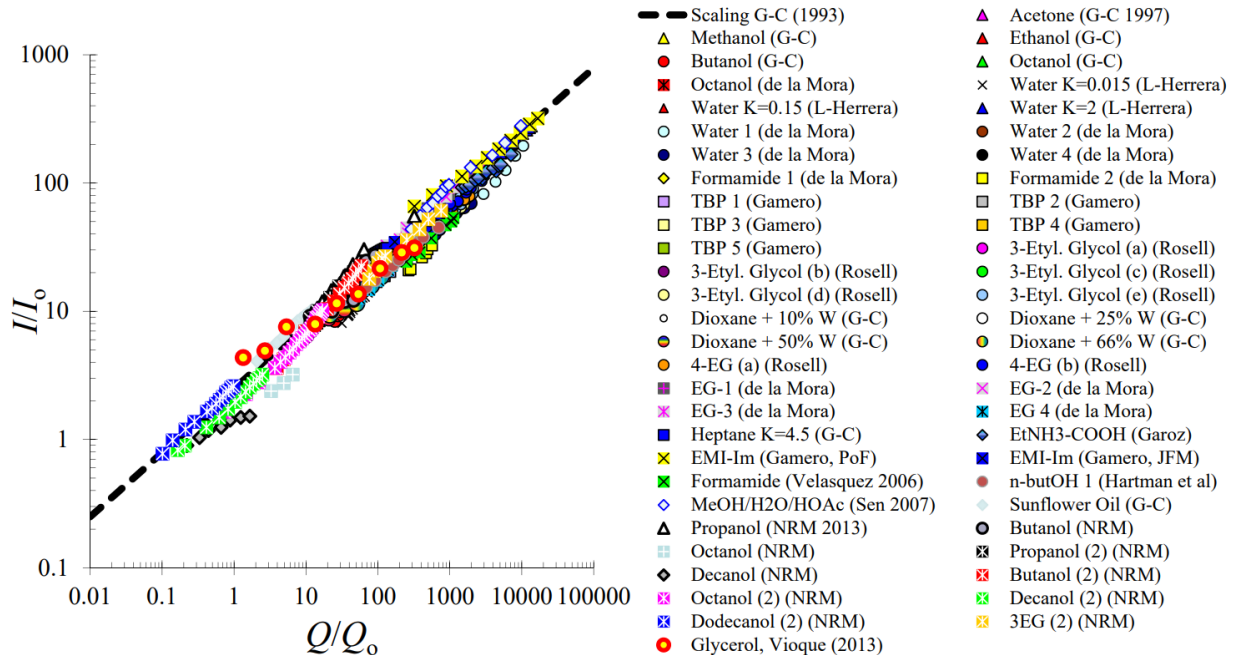


Figure 16. Electric current intensity I measured by different authors [17]

2.5 Uncertainties of the Instrument

The International Society of Automation (ISA), an international organization dedicated to the development of standards for automation, has a worldwide respected and practiced standard for symbology terminology and identification for instrumentation . Because of this, the bellow numbers were followed to obtain a pattern in the measurements and the uncertainties of the associated instruments and then, generate reliable diagrams later.

1. Recognize the desired inputs (measured), interferences and modifiers (influence quantities). It can be seen in the Figure 17.
2. Decide which influence quantities cannot be ignored in the specific application of the instrument.
3. Prepare the measurement procedure and trying to implement an exemplary method.
4. Calculate the standard uncertainty associated with the corrected indication of the instrument [24]. Considering only uncertainty propagation due to the error of estimation error of the parameters "a" and "b", assuming that "m" experiments were performed, we have the Standard Uncertainty associated to the Corrected Indication:

$$X = \frac{Y - b}{a} \quad (12)$$

$$u_{x_c} = \sqrt{\left[\frac{\partial f}{\partial x} \cdot u \right]^2 + \left[\frac{\partial f}{\partial b} \cdot s_b \right]^2 + \left[\frac{\partial f}{\partial a} \cdot s_a \right]^2} \quad (13)$$

$$X = \frac{Y - b}{a} + u_{x_c} \quad (14)$$

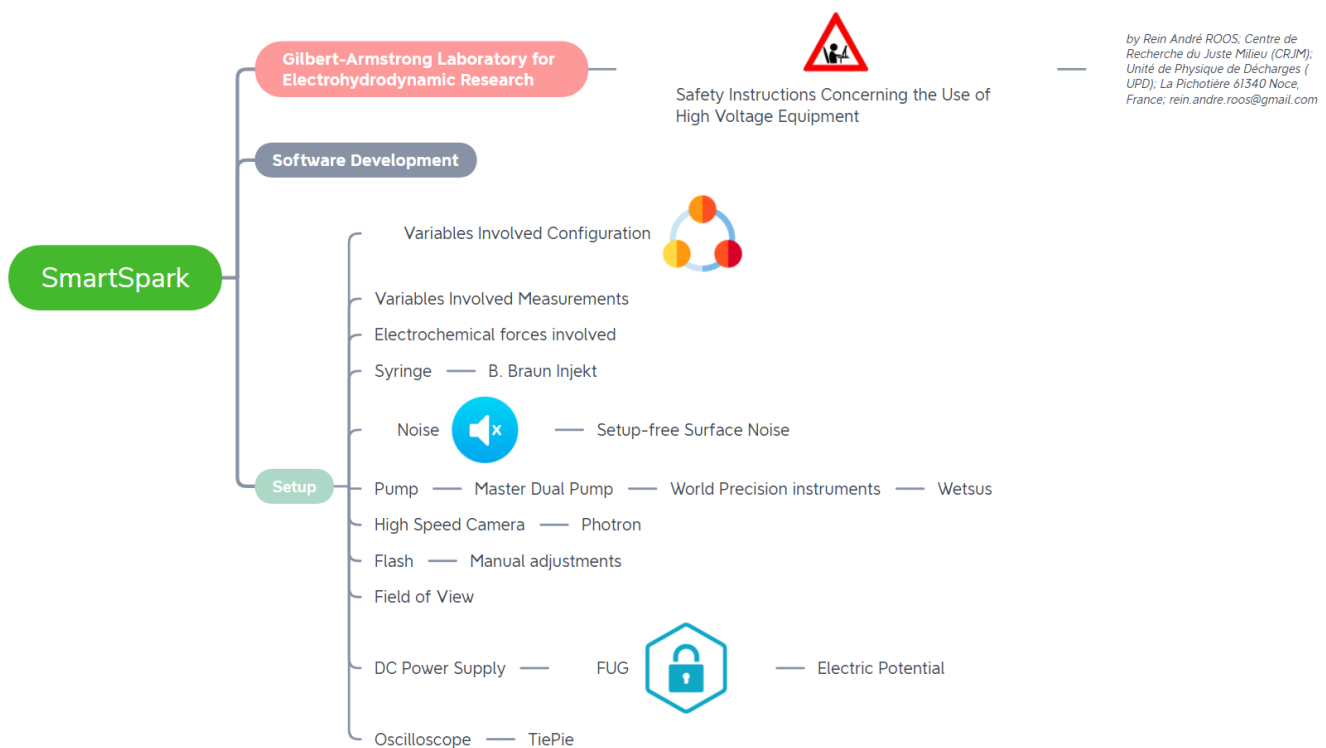


Figure 17. Setup instrumentation

5. Obtain the static characteristic curves (more than one) corresponding to each case for values of the influence quantities that will inevitably exist in the specific application application of the instrument.

2.6 First Electrospray Protocol

The first experiment routine was not automated. In all experiments the flow rate and electric potential configuration, for each liquid, was defined following the experiments done by Chen and Pui et al. (1997) [4] in the following way.

Firstly, the conditions to achieve a stable (cone-jet) mode was stabilized (flow and potential), after that the flow was kept constant and the potential was change in order to achieve other sprays modes (dripping, intermittent and multi-jet). We tried to keep the voltage constant until reach the cone-jet. The electric current was monitored in the ground line with a WiFi oscilloscope (TiePie Engineering). To monitor the spray type, a high speed imaging system was used with backlight illumination and a microscopic lens (Navitar x125). The camera was triggered manually.

Secondly, the HVPS was applied to the nozzle while keeping the counter electrode grounded. The first validation approach of the obtained electric current values (inside the cone-jet mode) was done using reference data [4]. After that, we used others references [11] [28], in order to collect data for different spray-modes and using different voltage regimes (step and ramp).

For each tested liquid (Ethanol, Ethylene glycol and 40 percent Ethanol with 60 percent Water) a specific flow rate is defined and a set of potentials is applied forcing the spray to run from the dripping mode until multi-jet. The voltage was not increased in a synchronized and timed manner. It is known that after a few seconds, the ES-mode can stabilize and this affects the spray dynamics. Therefore, it is very important that the data is collected in a timed and standardized way.

For each liquid, there is an operational window relative to the flow rate and the voltage applied where the cone-jet mode could be reached. Therefore, it was first important to fine-tune these variables until a stable cone-jet was visually reached. To achieve a stable balance, we used the minimum flow rate related to the literature and multiplied by 10^3 in order to get a nice range of spray-mode shapes.

To analyze the current, the current was being checked by the TiePie software, which shows the current values in data blocks. From the data block, the average was chosen and according to the uncertainties of the instrument the table below was made only for cone-jet values.

During the time window where the potential is shifted, the electric current values are acquired and treated continuously. ES was done with different solutions and under varied flow rate and voltage conditions.

2.7 Project Activities

Implementation of the software development was based on the figure 18 indicated bellow. The first step, known as the requirements, is important in order to assess what we need. Once this is complete, we will move on to the design stage where it will be created a blueprint of the system. After the design stage comes the implementation stage, which is where the system is actually built. Following this is the testing stage, where any errors or bugs are fixed. And finally, the system is deployed and put into use.



Figure 18. Lifecycle software

We made the analysis of requirements from the study of the technique and process previously shown in this work. From this, we observed all the variables involved in the process and divided so that each class and subsystem of SmartSpark is responsible for a function. This division of variables was shown in the diagram of the figure 19

The initial requirements of the program are related to the setup configuration, the properties of the liquids and from this, we can use the system to have a model to follow. This model was based on the publications previously shown, through statistical techniques and signal analysis, we have the output of the classification. From that, we can automate the system in real time.

2.8 Design

We evaluated the essential hardware and software components, networking capabilities, and processing and procedures needed for the system to achieve its goals during the Design. Since we know that the main goal of this project is to get closer to a fully automated control of the spraying process, we measured the properties of the liquid of interest and the setup geometry.

In order to do this, liquid properties are included in JSON files, which defines the properties of liquids: 1) surface tension; 2) dielectric constant; 3) viscosity; 4) density; 5) electrical conductivity.

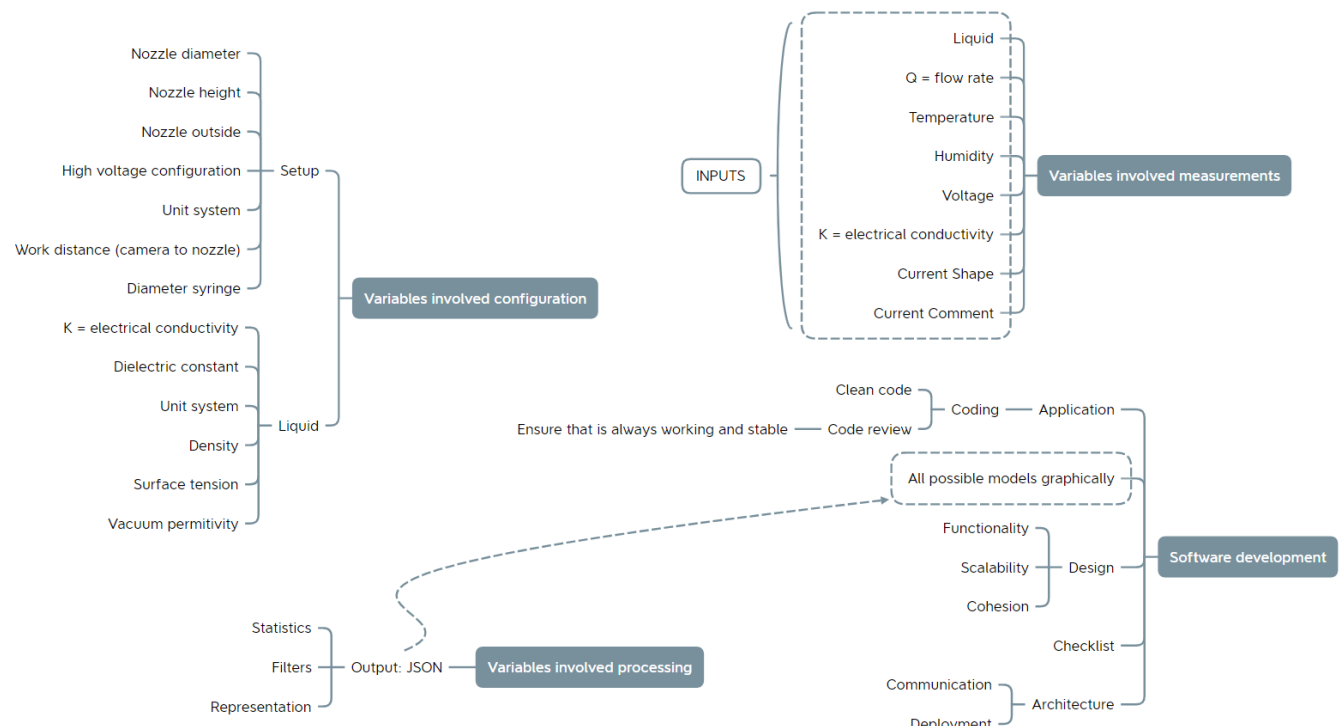


Figure 19. Variables SmartSpark (*variables software*)

They are all given in SI units. There is a setup folder with JSON files about the setup and contains information about 1) nozzle color; 2) camera and nozzle distance; 3) nozzle-to-plate or ring distance; 4) syringe inner diameter; 5) syringe outside diameter; 6) syringe height; 7) configuration (nozzle-to-plate or nozzle-to-ring); 8) high voltage (oscilloscope on the nozzle to plate for ex.); 9) syringe diameter; 10) coflow gas type; and 11) units.

In parallel, the Electrospray library was created in a manner that we could analyse offline and real-time measurements. There is a JSON folder with JSON files for tests purposes, a literature folder with files with a lot of matplotlib plots for diagrams purposes, offline treatment folder with non real time process with code for offline treatment.

Furthermore we have a Tiepie configuration file with communication with oscilloscope control, serialFUG folder with power supply FUG control commands , serialpump folder with pump control commands and useful commands for controlling the pump, viewer folder with a viewer class that loads saved data in JSON and visualizes (plots) it, including Fast Fourier Transform. Threads were done in order to maintain the system working between the controlling of the HVPS and the data treatment system.

2.9 Current Measurement

Even small currents involve a great number of electrical charges. Current in the μA level are some $1\text{e}12$ elementary charges passing per second. Currents involved in electrical discharges vary over a very wide range.

In order to measure current with an oscilloscope, the oscilloscope should be connected in series with the circuit. This will allow the oscilloscope to measure the current flowing through the circuit. The ground clip of the oscilloscope probes must also be connected to a known ground point in the circuit.

There is a requirement list for current measurement: 1) current range to measure is from 1 nA to 5 μ A in the spray-modes; 2) it depends in one particular setup/experiment; 3) when the power supply is switched off, charges from the nozzle can flow back towards the output capacitor burning resistors of the power supply.

To collect the electric current data sampling rates of 100 kSps (kilo samples per second) are sufficient considering the upper bandwidth limit of 3,5 kHz of signals documented in literature [28] (but also confirmed by measurements). Usual sampling settings are 50 kS (kilo samples) at a sampling rate of 100 kSps resulting in blocks of data representing 500 ms. For each block the mean and RMS values, standard deviation, and FFT and power spectral density are calculated. The results are further used for automatic classification of the spray.

There is an integration between the TiePie Oscilloscope and the code developed. This occurs due to the Tiepie Python library. There is an $1\text{ M}\Omega$ input resistance when in single ended input mode and $2\text{ M}\Omega$ default input resistance when is the differentiate mode. The differentiate mode was the most used. All the datapoints or values collected in the oscilloscope are multiplied for 500 and the explication is on see following equations from 15 until 18.

$$U = R \cdot I \Omega. \quad (15)$$

$$U = I \cdot 2\text{ M}\Omega. \quad (16)$$

$$I[A] = \frac{U}{2 \cdot 10^6 \Omega} \quad (17)$$

$$I[nA] = \frac{U \cdot 10^9}{2 \cdot 10^6 \Omega} = U \cdot 500 \quad (18)$$

Regarding to the programming language, a major practical consideration when using Python is its speed, but in this system the performance in order to manipulate discharges was sufficient. Besides this, the execution of the work allowed visualizing that Python would not be the best language for applications that demand a high degree of speed, because it is not fast and the processing time is big.

Moreover the measurement resistance was always intentionally kept relatively small to minimise its influence on the spraying behaviour. One measurement is 500 ms. 600 measurements of 50 k samples with 100 kHz (sampling frequency equals to 10^5) equals to 5min. The record length is 50000 samples. The trigger time out is 100e^{-3} s, or 100 ms.

When the input range is e.g. 8 V, signal values between -8 V and +8 V can be measured. Values outside that range will be clipped. The range pre-define is -4 V and +4 V and it was defined based on the first ES protocol in the first sub chapter of this method section. This code configures a TiePieScope object, setting the sampling frequency, record length, and trigger settings.

```
import libtiepie

def config_TiePieScope(scp, sampling_frequency):

    # input impedance by default is 2MΩ in differential mode
    scp.measure_mode = libtiepie.MM_BLOCK
    scp.sample_frequency = sampling_frequency
    scp.record_length = 50000
```

```

scp.pre_sample_ratio = 0
scp.channels[0].enabled = True
scp.channels[0].range = 4 # range in V

scp.channels[0].coupling = libtiepie.CK_DCV # DC Volt
scp.channels[0].trigger.enabled = True
scp.channels[0].trigger.kind = libtiepie.TK_RISINGEDGE
scp.channels[1].enabled = False
scp.channels[2].enabled = False
scp.channels[3].enabled = False
scp.trigger_time_out = 100e-3 # 100 ms

# Disable all channel trigger sources:
for ch in scp.channels:
    ch.trigger.enabled = False

# Setup channel trigger:
ch = scp.channels[0] # Channel 1 in the tiepie
# Enable trigger source:
ch.trigger.enabled = True
ch.trigger.kind = libtiepie.TK_RISINGEDGE # Rising edge
ch.trigger.levels[0] = 0.5 # 50 %
ch.trigger.hystereses[0] = 0.05 # 5 %
return scp

```

2.10 Protocol Measurement

This protocol measurement are the routines of the automated measurement and it will be explained numerically.

1. For each tested liquid a specific flow rate is defined based on the cone-jet minimum flow rate and a set of potentials is applied forcing the spray to run from the dripping until multi-jet mode.

1.1. The minimum flow rate of the system is defined as the product between surface tension and vacuum permittivity, divided by product between density and conductivity as follow the equation 19.

$$Q_o = \frac{\mu \cdot \epsilon_0}{\rho \cdot K} [m^3/s] \quad (19)$$

1.2. For practical reasons and to stabilise the cone-jet for a longer time, the minimum flow rate values was multiplied by 10^3 and the experiments were started from there.

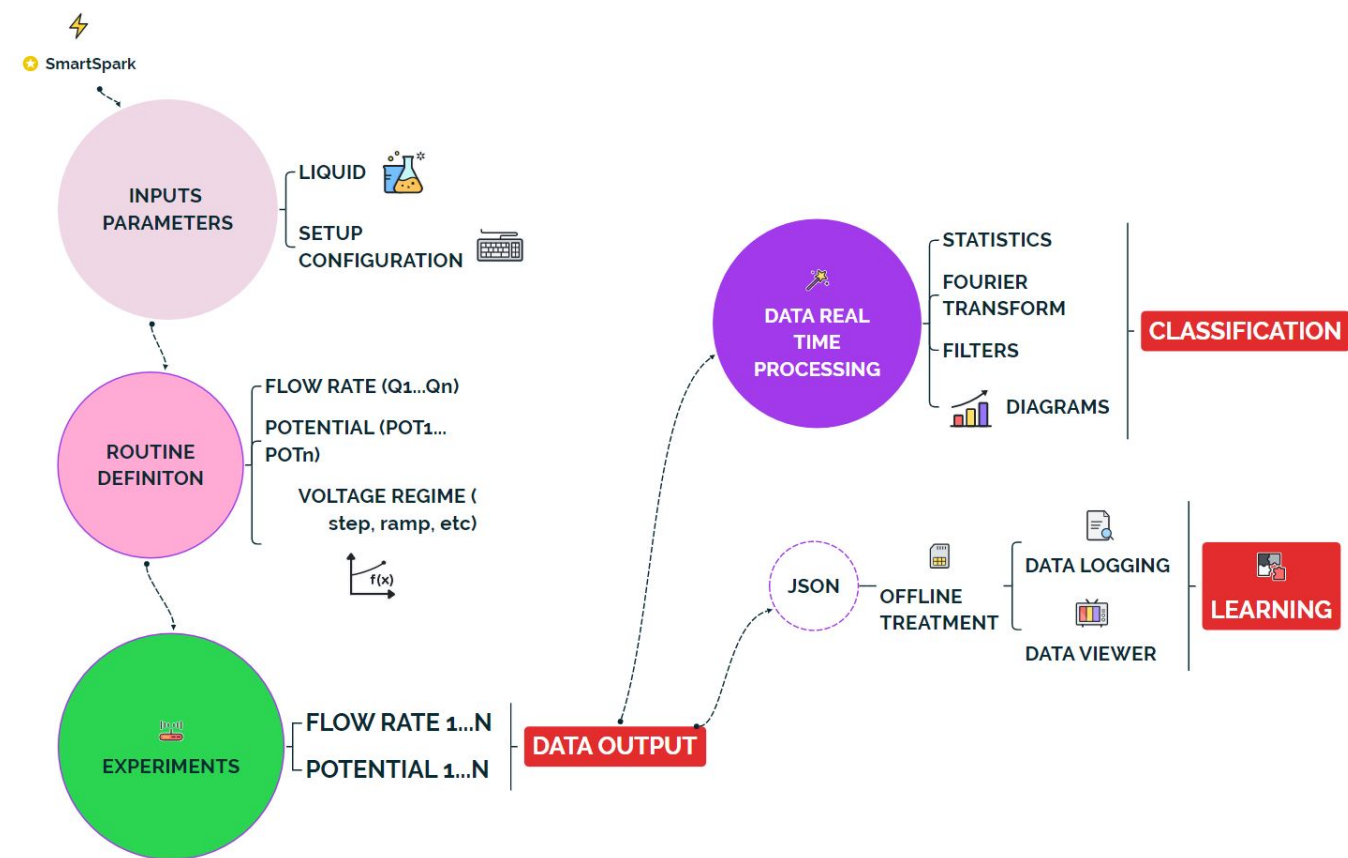
2. During the time window where the potential is shifted, the electric current values are acquired and treated continuously.
3. Many digital signal processing techniques and statistics are applied to the data immediately after acquisition, e.g. Fourier Transform, mean value, standard deviation, mean value, etc.
4. The Python program correlates the treated values of the electric current with a specific voltage regime (step, ramp, etc) and different plots can be generated relating the current values with a specific potential window.
- 4.1. The method to collect data changed the voltage regime into steps and ramps sequences in order to change the voltage for a range between the spray-modes dripping and multi-jet. The region after multi-jet was taken into account because we want to verify the region of the sparks in the EHDA system.
5. Using the variables proposed by [28] the program checks the electric current values and automatically identify which mode is running at a certain voltage-flow rate window.
6. To validate the mode classification proposed by the program a high speed camera imaging (Photron with a Navitar 125x microscopic lens) system runs in parallel doing screenshots to the experiment providing continuous monitoring of the ES modes. This is not synchronized.

2.11 Flow of Information in the SmartSpark

The electric current is flowing through the oscilloscopes input resistance and the system is assuming current ranges of 1 nA to $1\mu\text{ A}$ resulting in voltage drop in the range of 2 mV to 2 V . The sampling rate is 100 kHz and the data blocks of 50 kS , which is equivalent of 500 ms as explained in 18.

The diagram below 20 is the flow used to explain how does the information is in the experiments. 1) Input Parameters: you fill in the initial parameters about the liquid and the setup configuration. 2) Routine Definition: you define what is the pump flow rate, the voltage range involved from the HVPS and what is the voltage regime (step, ramp, step size, etc). 3) Experiments: where you start the experiments and there is an output from the WiFi Oscilloscope. 4) Data Real Time Processing: applies statistical techniques, FT, low-pass filters and forms a diagram. From this there is a classification.

From the output of the oscilloscope, we also have the opportunity to view and log in offline so we can check the operation of the code and verify that the classification is correct.

**Figure 20.** Flow of data

2.12 Data Processing

Since we have the Wifi Oscilloscope from Tiepie Engineering integrated in the system in real time, digital signal processing and statistics were applied in the data. We divided the class with its functionality based on the 21.

JSON is easy to read and write and it is a lightweight text-based interchange format that is programming language independent. If in the future we want an embedded equipment in C++ it would be easy, for example. It supports a wide range of data types, making it suitable for use in a wide range of applications.

Each saved file has setup data, liquid properties and measurements. Every measurement has 50.000 data points and for each measurement a lot of information based on digital signal processing techniques and statistics of the current data were done.

2.13 Statistical Analysis

Some terms from Statistics are important in the ES system for the non-visual classification. The mean value represents the signal's DC content, which is the center tendency best if data points are symmetrically distributed above and below the mean, hence no outliers. The median value is less

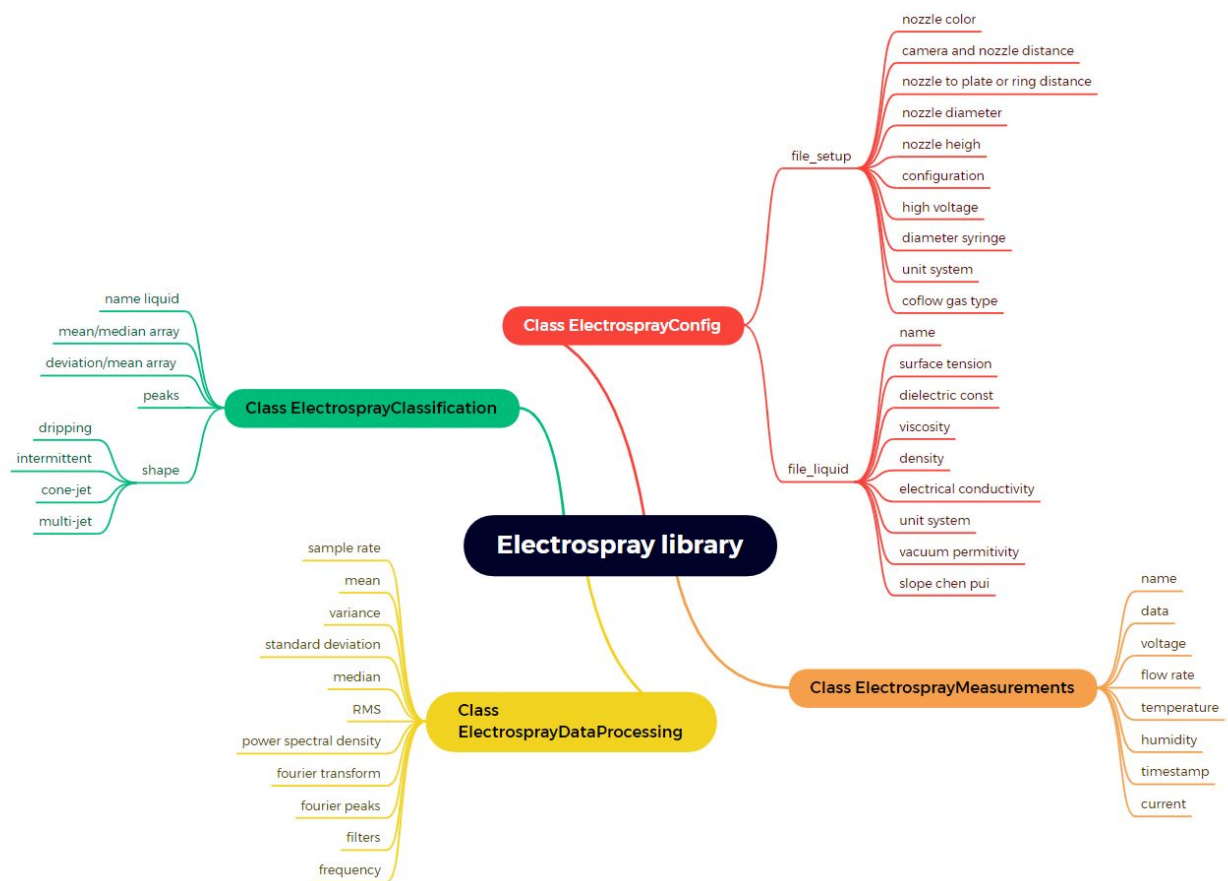


Figure 21. Library diagram

sensitive to outliers. The mean and standard deviation represents the signal to noise ratio and it also represents the AC Power content of a signal.

The Root Mean Square (RMS) is the sum of DC and AC signal power content. Mean-square in electrical terminology is often referred to as the average power (from the notion that the mean-square value of a voltage or current waveform, applied to $1-\Omega$ resistor, gives the average power dissipation in watts) [16].

The variance is therefore similar to the mean-square, but with the mean removed. It follows that the variance is a measure of the average powers in all its other frequency components. The variable mean divided by standard deviation is the signal to noise ratio [16].

There are some variables used by [28] to classify the spray-modes that will be shown in the figure 22. In this section, we show the variables defined by his papers and we included our own method of classification in further chapter.

Configuration 4 type III is: the nozzle-to-plate configuration; the needle type has the outer diameter of a capillary ((d_{cap})) = 2.00 mm; the inner diameter of a capillary ($(d_{cap}),_{in}$) = 0.20mm; distance from capillary and the plate (L_p) = 15mm; Resistance = 11460Ω . We can see that the nozzle type have an inner diameter of 0.2 mm which is significantly smaller than (d_{cap}) for the nozzles used in the current experiment [27].

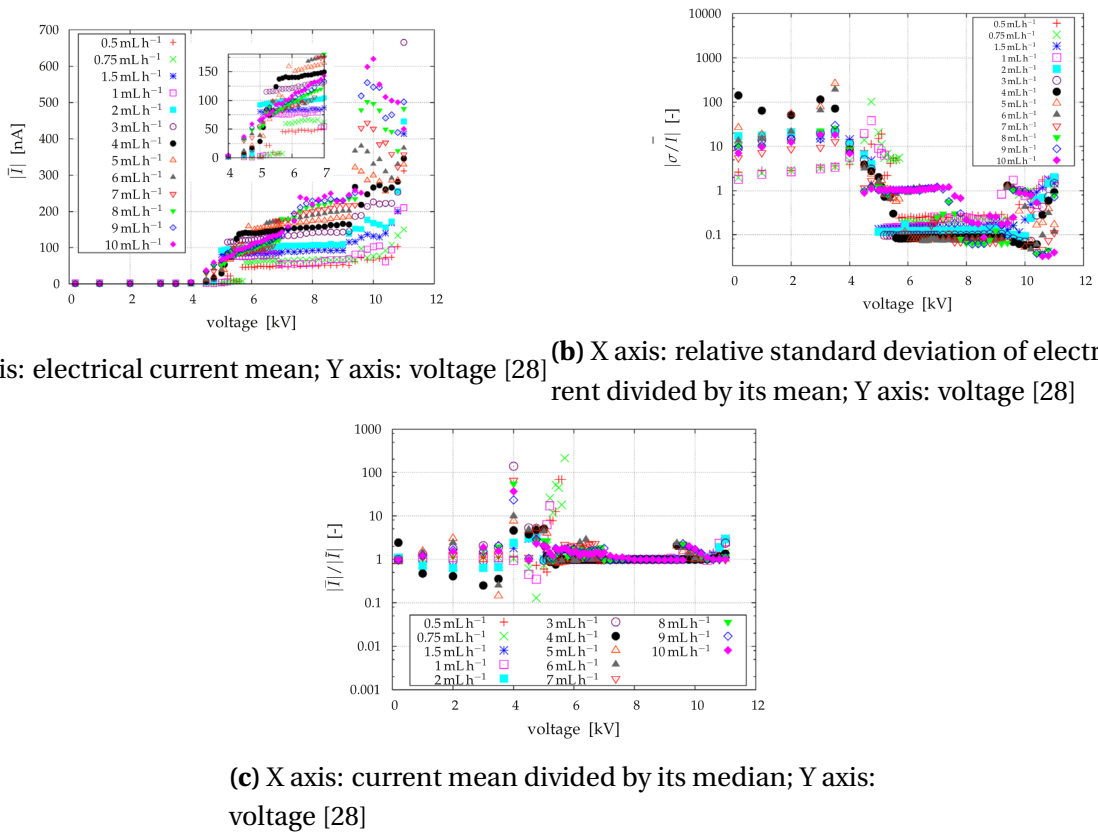


Figure 22. Typical processing results for the characteristics of Sections 4.1 and 4.2 for a configuration 4 (Type III) system spraying ethanol. [28]

2.14 Digital Signal Analysis

A signal is information that changes over time. For example, audio, video, and voltage traces are all examples of signals. A digital signal is a signal that is sampled at some regular interval, and then the samples are quantized. The digital signal can be either an analog signal that has been converted to a digital signal, or it can be a digital signal that has been generated by a digital device.

The process of digital signal analysis is the process of analyzing a digital signal in order to extract information from it. The information that can be extracted from a digital signal depends on the type of signal that it is. For example, a digital image can be decomposed into its constituent pixels, and the color and intensity of each pixel can be analyzed. Likewise, a digital audio signal can be decomposed into its constituent samples, and the amplitude and frequency of each sample can be analyzed.

Digital signal analysis is a powerful tool for extracting information from digital signals. It can be used to analyze signals in order to extract information about the underlying physical phenomena that generated the signal. Additionally, digital signal analysis can be used to improve the quality of digital signals. For example, digital signal analysis can be used to remove noise from a digital signal.

The Fourier Transform (FT) is a powerful tool that is used in many different fields, from signal processing to data analysis. The FT of a signal is a representation of the signal in the frequency

domain. It can be used to find the frequencies that make up the signal, and to analyze how those frequencies change over time. Fourier transforms (FT) is good for analyse the spectrum (angle and phase and magnitude) of the signal. This is done via array to map the points from the FT.

Every time-domain functions has a counterpart in the frequency domain. In the case of an auto-correlation function (ACF) which is a function of the time-shifted variable m , the counterpart is called a power spectrum density or, more simply, a power spectrum. It indicates how the sequence's power or energy is distributes in the frequency domain, and is widely-used measure of random signals and noise [16].

One variation of the FT that is used when the signal is discrete, or digital is the Discrete Fourier Transform (DFT). The DFT is a powerful tool for analyzing signals and determining the frequencies that make up the signal. The DFT is a mathematical transformation that converts a signal from the time domain to the frequency domain. The DFT is used in many signal processing applications, such as filtering, equalization, and compression. The DFT can be used to determine the frequencies of a signal, as well as the amplitude and phase of each frequency component. The DFT is a valuable tool for analyzing signals that are not periodic, such as noise. The DFT can also be used to analyze signals that are periodic, but have a complex waveform, such as speech or in our case, an EHDA spray-modes signal and also sparks regions.

Highly efficient algorithms for computing the DFT were first developed in the 1960s. Collectively known as Fast Fourier Transform (FFTs), they all rely upon the fact that the standard DFT involves redundant calculation. It is the aim of Fast Fourier Transform (FFT) algorithms to eliminate the redundancy through the decomposition of a DFT into successively shorter DFTs. [16]

For doing the calculations, NumPy was used mostly. Numpy is a Python library for scientific computing. It provides a high-performance multidimensional array object, and tools for working with these arrays. Numpy is free and open-source software released under the three-clause BSD license. Numpy is a powerful tool for digital signal analysis. It is able to process large amounts of data very quickly, making it an essential tool for anyone working with digital signals. Numpy also has a wide range of functions for signal processing, making it a very versatile tool.

The FT is a tool that is used extensively in the Python library NumPy and it is a fundamental tool in many different areas of science and engineering. NumPy provides functions for computing the Fourier Transform of a signal, and for inverse Fourier Transform as well. NumPy also provides tools for working with signals in the frequency domain, such as filtering and windowing. For more: <https://docs.scipy.org/doc/scipy/reference/tutorial/fft.html>

Frequency-selective filters attempt to exactly pass some bands of frequencies and exactly reject others. A low pass filter is a filter that allows low frequency signals to pass through while attenuating high frequency signals. Frequency-shaping filters more generally attempt to reshape the signal spectrum by multiplying the input spectrum by some specified shaping. Ideal frequency-selective

filters, such as lowpass, highpass, and bandpass filters, are useful abstractions mathematically but are not exactly implementable.

Many simple, commonly used approximations to frequency-selective discrete-time filters also exist. A very common one is the class of moving average filters. These have a finite-length impulse response and consist of moving through the data, averaging together adjacent values.

First, we analyse one measurement of 50.000 data points which has the current signal. If the maximum value of this data is greater than 1500 Volts, and the flow rate is less than 100 micro liters per hour, and the percentage of the maximum is greater than 0.05, or the quantity of maximum of the data is greater than 20.000 (in the 50.000 data points of one measurement), then it returns "streamer onset." If the flow rate is greater than 100 micro liters per hour, and the percentage of maximum is greater than 2, or the quantity of maximum data is greater than 20,000, then it returns "streamer onset." If the maximum value of the data is not greater than 1,500, it returns "no streamer onset."

Secondly, the code verifies the Fourier peaks by frequency and amplitude, and classifies as "maximum peak" if they are above 50 Hz and greater than 1500 Volts. After that, if the flow rate is less than 200 micro liters per hour, and the peak count is greater than 5, it is classified as "streamer onset". If the flow rate is greater than 200 micro liters per hour, and the peak count is greater than 10, then it returns "streamer onset."

2.15 Viewer

A viewer class was created and it can be seen in the figures 23 and 24. It allows visually browsing through blocks of data and manually verify and correct classifications. These data sets can further be used to train a neural network for an alternative classification approach.

Furthermore, we can see in the figures 23 and 24 we show the classification made by the system automatically, as well as the number of the measurement, average, rms, power supply current, power supply voltage, standard deviation and also the median of the program. This facilitates the knowledge creation later on.

Finally, the viewer class ensures that the JSON chosen by the user is loaded and that we can scroll through the data collected via the oscilloscope. The "prev" button goes to the previous measurement and the "next" button to the next measurement in a dynamic function. It allows visually browsing through blocks of data and manually verify and correct classifications.

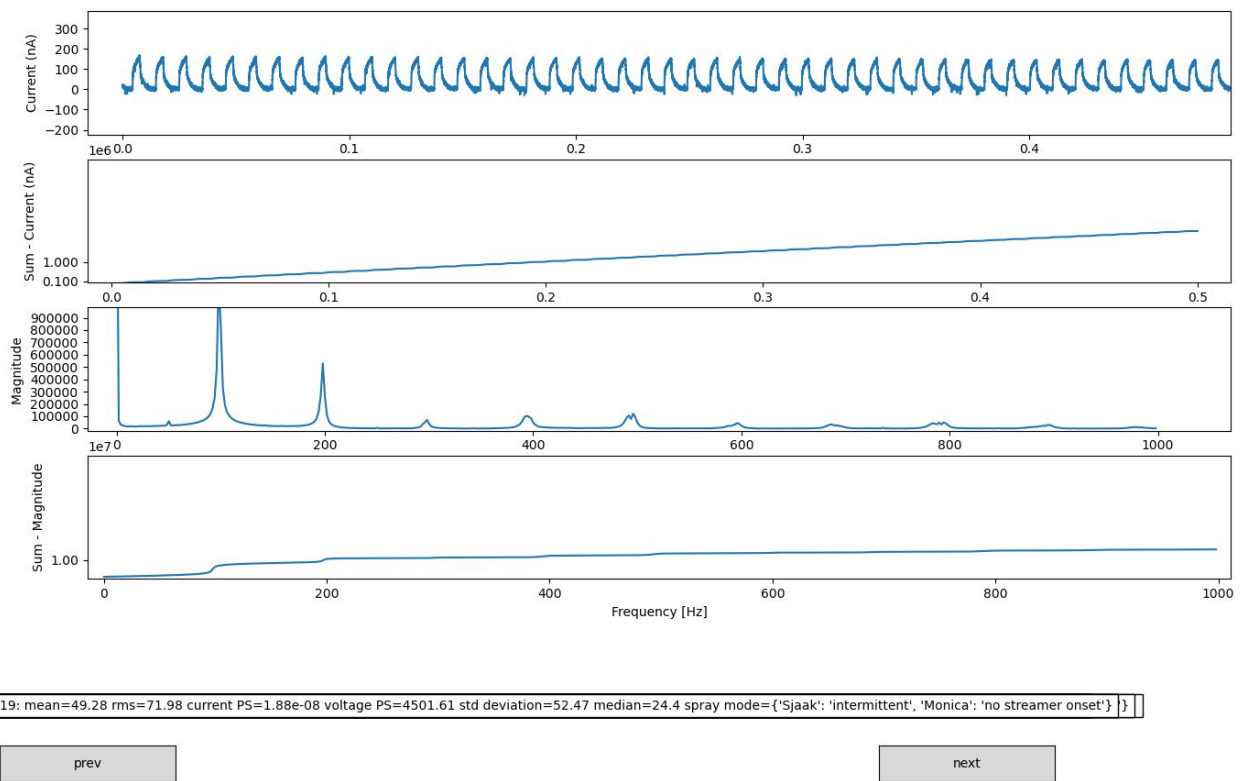


Figure 23. Viewer in the spray-mode intermittent

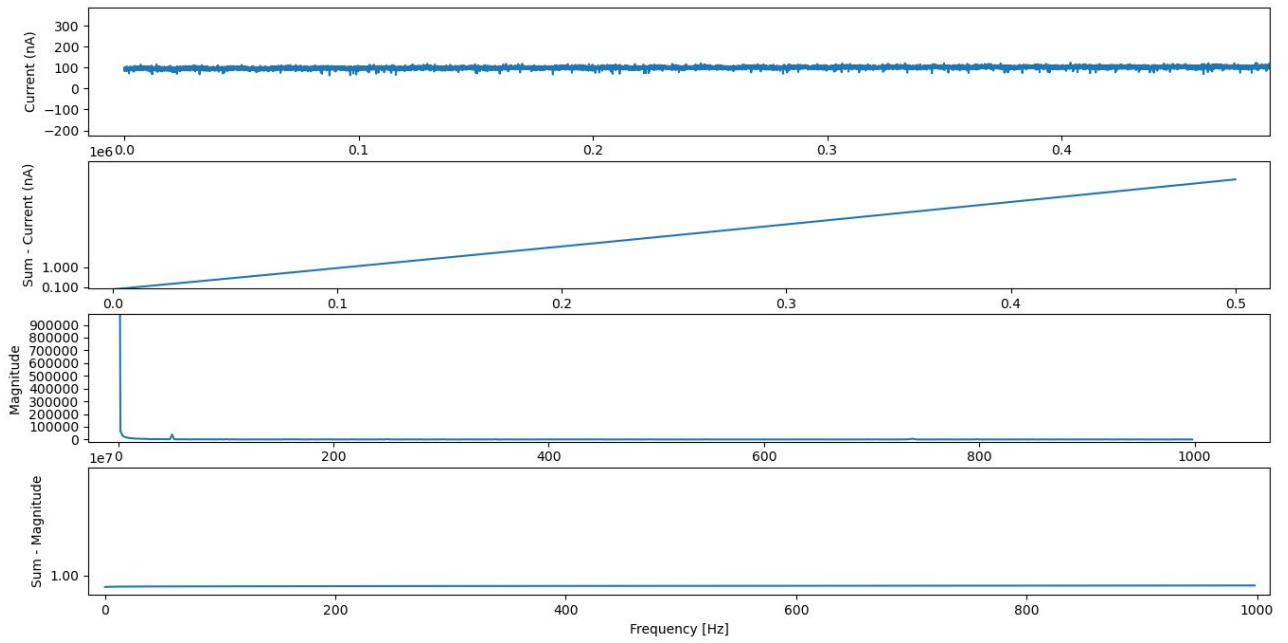


Figure 24. Viewer in the spray-mode cone-jet

2.16 SmartSpark Development

1. Use of the system: for the experiment to be done, it is necessary to have knowledge about the ES technology from the publications made and after that, study of security to deal with high voltage equipment.
2. Processing: the system does the processing about the information with the variables set in the main file. To change it, you should verify the sample rate of the oscilloscope on it. We use a block mode from the open source library in the Tiepie engineering github.
3. In order to have the integration with the HVPS, the configuration was made on an Windows PC with SO of 2007, following the manuals of its website and with the Baud rate of 115200. This information can be useful in further development. Threads were done in order to maintain the system working between the controlling of the HVPS and the data treatment system.
4. In order to have the integration with the PUMP-AL-1000 NE-100, the software PumpSeryingePro was bought. The serial commands were studied via serial commands trackers softwares to learn the correct order of the serial commands.
5. Information about the liquid properties was collected.
6. The system was made in a way that the variables, class, objects and all the information collected has names that you can easily identify and read and it is most used the Standard Units patterns for all the measurements.
7. Commands are sent via terminal Python. We used an i7 machine with Windows SO and in the PyCharm Community software to do all the automatic measurements and tests.
8. While the user is running the system, a display in real time with the 50.000 datapoints of the electrical current signal will be shown. With this block of data we have also in the same window of the signal the following variables and treatment: 1) mean, 2) standard deviation, 3) fast fourier transform, 4) percentage of peaks in the fast fourier transform, 5) classification based on the paper [28].
9. After the end of the program, we have the JSON structured in a readable way and we can use this data with the viewer class.

2.17 SmartSpark System Protocol

To use the library in the High voltage lab you need to follow the steps bellow:

0. Be part of the contributers in the github repository url: <https://github.com/emediato/electrospraylib>.
1. Open the file: mainelectrospray_fug_allshapes.py

2. Verify the file that is indicated in the variable "name_setup" in the url indicated in the variable "setup".

2.1. The "setup" indicates the url of where the file is located.

2.2. Open this file.

3. Verify if the properties of the setup like "nozzle color", "camera to nozzle distance", "config", "nozzle-to-plate or ring distance", "nozzle diameter", "nozzle outside", "nozzle height", "high voltage", "diameter syringe", "units", "coflow gas type" is the same as in the 2.1.

3.1. If not, create a JSON file in the "setup" folder with all the information and change the assignment string of the variable "name_setup" with the file created.

4. Verify the file that is indicated in the variable "name_liquid" in the url indicated in the variable "liquid" url.

4.1. The "liquid" indicates the url of where the file is located. Open this file.

4.2. You need to know which liquid you are dealing.

5. If you would like to save all the information, the boolean assignment of the "VAR_BIN_CONFIG" should be = TRUE. If not, = FALSE.

6. If you would like to have a voltage regime of RAMP, the boolean assignment of the "MODERAMP" should be = TRUE.

6.1. The RAMP mode is combined with the arbitrary assigment " number_measurements = 50 " because it is a good size for saving.

6.2. The line from 221 until 226 indicates the information about txt_mode, slope, voltage_start, voltage_stop, step_size=0 and step_time=0.

6.2.1. Step_size and step_time = 0 because it is in the ramp mode.

6.3. Be sure that there is only one variable "number_measurments" assigment.

7. If you would like to have a voltage regime of STEP, the boolean assignment of the "MODERAMP" should be = FALSE.

7.1. The STEP mode is combined with the arbitrary assigment " number_measurements = 100 " because it is a good size for saving.

7.2. The line from 208 until 213 indicates the information about txt_mode, slope, voltage_start, voltage_stop, step_size and step_time. Very intuitive what this means.

8. To set the flow rate you can do in the software SyringePumpPro (see Figure 25) or manually in the pump (see manual).

8.1. Verify if the flow rate (in the same file as 1) in the float variable assigment " Q = " is the

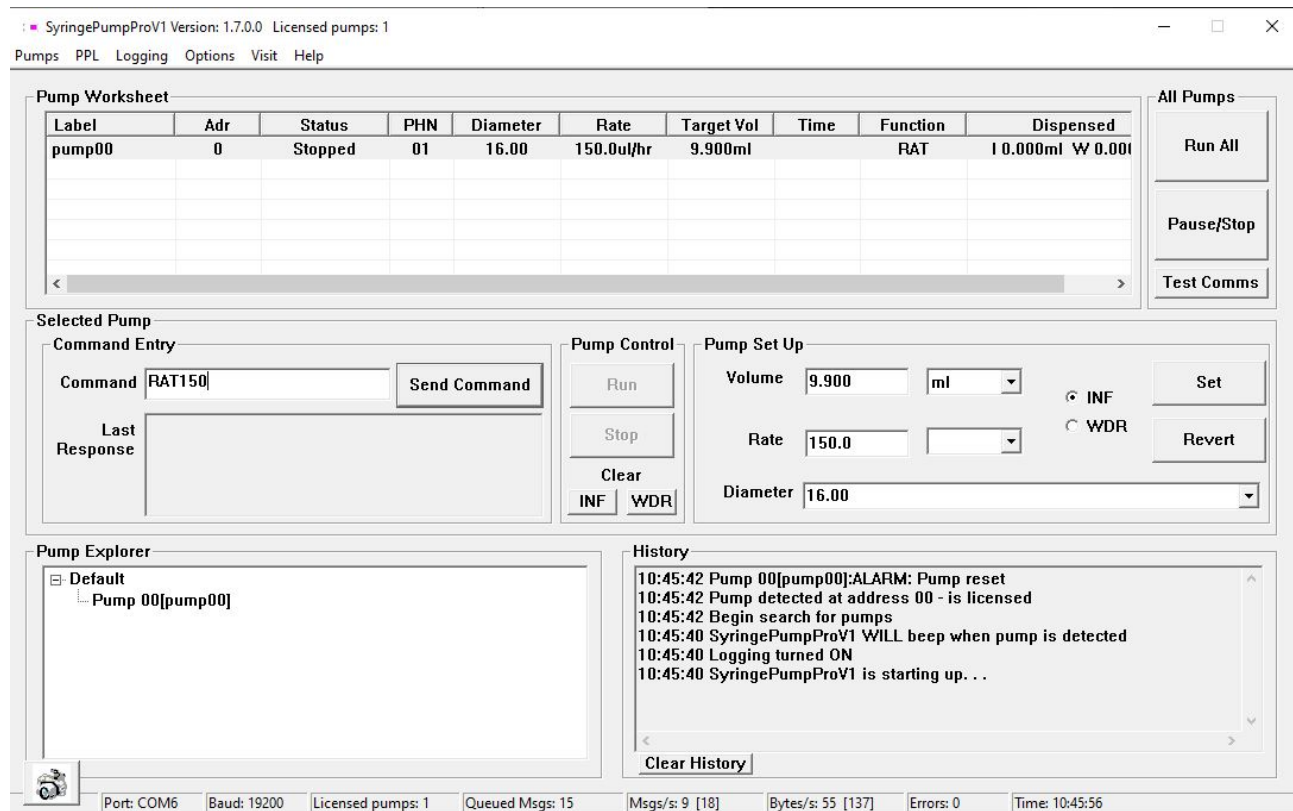


Figure 25. Set the flow rate in the command [Nair] (SyringePumpPro)

one that you set. Make sure it is uL/h.

8.2. Useful commands for pump, for more check the manual of the SeryngePumpPro:

ADRO

RAT5.0 [uL/h]

BUZ5

VER

8.3. Do not format the PC or you will lose the license of this software.

9. Verify if the path is the one that you would like to save in the variable "save_path".

10. Run the file defined in 1.

A summary of the steps was created in a timeline way and the numbers of this list are indicated in the figure 26.

2.18 GasUnie B.V. Implementation Networks

In order to realize the electric current monitoring system in a natural gas company (see Figure 27), the configuration of a web server to log the information was necessary. The ES system will be underground and we cannot visualize the system. Knowing this, we developed a data logger

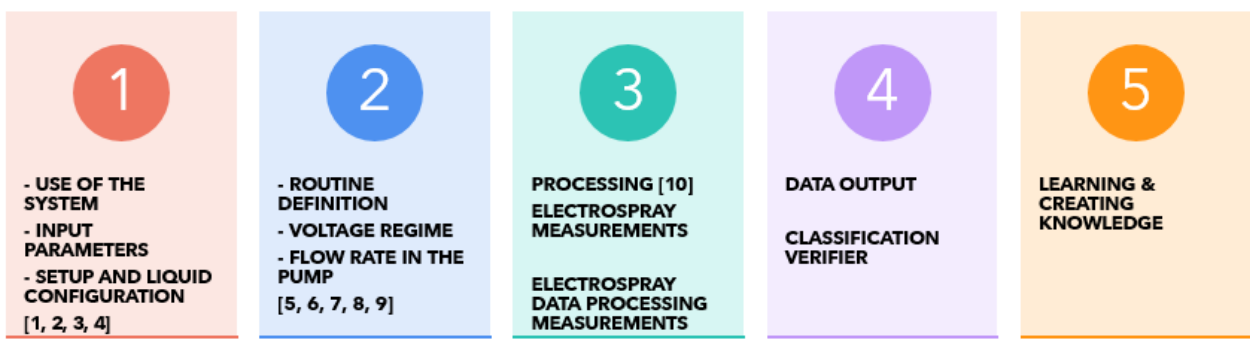
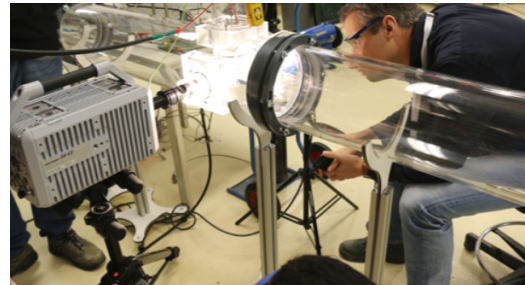


Figure 26. How to start the system [Nair] (*Step by step*)



(a) Implementation at GasUnie of the ES system



(b) Transparent tube for testing the ES system

Figure 27. Tests GasUnie

to monitor the electric current of the system. From ancillary experiments, we know that the Gas Odorization System works between cone-jet and multi-jet.

The Raspberry Pi 4B was the device chosen to conduct the data logging. In a computer with Windows operating system (OS), the "Putty" software was used to communicate with the equipment via Secure Shell (SSH) and the software "WinSCP" to write, read and copy files between computers using communication protocols: FTP, FTPS or SFTP. In a Linux OS the terminal has been used to do the same relationship between machines.

GasUnie's design requires the oscilloscope to be on the high voltage side. In other words, the oscilloscope is in series with the power supply and the electrospray nozzle. Figure 28 shows a sketch of the electrical circuit. The high voltage cable is connecting the nozzle to the High Voltage (HV) Power Supply and the TiePie Oscilloscope. In order to make the connection between instruments, it was necessary to make a small box so that the current was in series in the nozzle and in the oscilloscope. The high voltage cable that came from the Power Supply was cut off and we made a tiny cabling box for it to run through the oscilloscope as showed (29) in the chapter 2.18. Tests were done with the oscilloscope on the high voltage side with this cable box. This was made with solder and a plastic material for laboratory testing purposes. For scale testing, a cabling company was hired.

We could have used our Raspberry Pi as a wireless access point, but we simply connected to the TiePie oscilloscope in a direct WiFi connection. To activate changes in the wpasupplicant file,

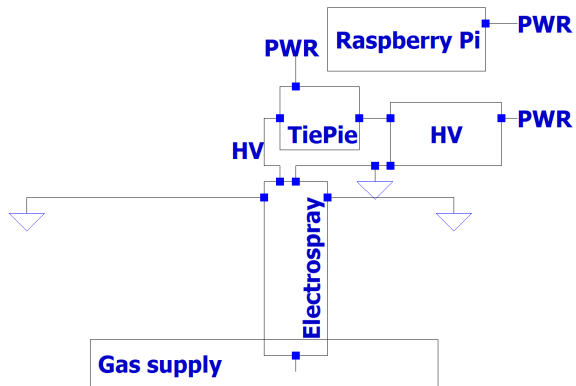


Figure 28. Electrical circuit for GasUnie. The diagram of the submerged ES system has not been drawn.



Figure 29. Cabling box

Raspberry Pi needs to restart. Connection with the oscilloscope was made in the wpasupplicant file of the network of the Raspberry Pi. The file has the code lines below:

```

network={

    ssid="TiePie-WS6D-37427"
    key_mgmt=NONE
}
    
```

To support all the libraries that involves the monitoring ES system, we used the virtual environments (venv) in the Raspberry Pi. "The venv module provides support for creating lightweight “virtual environments” with their own site directories, optionally isolated from system site directories. Each virtual environment has its own Python binary (which matches the version of the binary that was used to create this environment) and can have its own independent set of installed Python packages in its site directories." [5] It is possible to have different versions of different libraries.

Besides that, in order to control the power supply with the Raspberry Pi, the configuration of serial interfaces must be done. The login shell must not be accessible and the serial port hardware must be enabled.

2.18.1 InfluxDB and Grafana

The logging for Domoticz and some of the associated automation services can be pretty heavy. SD cards do not perform optimally when you write – and overwrite – lots of data [Durdle]. It is important to know specifications about swap, noatime flag of the Raspberry, because there is always a risk of burning the SD card.

To do the logging and monitoring system in a Gas Odorization System, we need a Time series database (TSDB). TSDB consists of measurements or events that are monitored, tracked, refinement of data i.e down sampling and aggregated over time. They can be application monitoring analysis data, server metrics, data about sensors, market trading data, stock exchange data across markets [Nair]. There are several time series database available, but which one is the most popular and the best for our purpose? The figure 30 answers this question. InfluxDB was the database we choose. There is a large community that makes use of it and that is positive. InfluxDB is a time series database designed to handle high write and query loads. InfluxDB is meant to be used as a backing store for any user case involving large amounts of timestamped data, including DevOps monitoring, application metrics, IoT sensor data, and real-time analytics.

RANK MAY 2022	DBMS	SCORE		
		MAY 2022	24 MOS ▲	12 MOS ▲
1	InfluxDB	29.55	+8.37	+0.91
2	Kdb+	8.98	+3.12	+0.66
3	Prometheus	6.13	+1.54	+0.21
4	Graphite	5.46	+1.83	+0.82
5	TimescaleDB	4.70	+2.52	+1.46
6	ApacheDruid	3.00	+1.05	+0.19
7	RRDtool	2.50	-0.40	-0.19
8	OpenTSDB	1.84	-0.19	+0.00
9	DolphinDB	1.65	+1.18	+0.69
10	Fauna	1.36	+0.17	-0.31

Figure 30. Why did we choose InfluxDB? [Nair] (*why InfluxDB*)

There are a number of languages out there that already have InfluxDB libraries, many of them maintained by the community open source [6]. We used influxdb-python library and like many Python libraries, the easiest way to get up and running is to install the library using pip. After the installation of the InfluxDB, The "influxd" command on the terminal of the Raspberry Pi must provide access to the database and SQL commands in the terminal like those ones:

```
show databases
create database <NameOfTheDataBase>
```

To connect to an InfluxDB, an InfluxDBClient object [7cb56569] must be created. The default configuration connects to InfluxDB on localhost with the default ports. The below instantiating statements are all equivalent:

```
from influxdb import InfluxDBClient

host = 'localhost'
port = 8086
username = 'admin'
password = 'admin1234'
db = 'testdb'

client = InfluxDBClient(host, port)
client = InfluxDBClient(host, port, username, password)
client.switch_database(db)
```

It is necessary to get acquainted with some key concepts of the database in its documentation. InfluxDB has a line protocol for sending time series data which takes the following form: measurement-name tag-set field-set timestamp in a JSON format. The following code shows how it is organized.

```
json_body = [
    {
        "measurement": "tiepie-rpi",
        "tags": {
            "classification": classification,
        },
        "time": timestamp,
        "fields": {
            "running_id": id,
            "std_current": std,
            "mean_current": mean,
            "voltage_PS": voltage_PS,
            "datapoints": datapoints,
            "temperature": temperature,
            "humidity": humidity
        }
    }
]
client.write_points(json_body)
```

For documentation as figure bellow we will see that: 1) Measurement: what you are measuring (it is conceptually similar to a table for SQL users) - usually a string; 2) Tag set: How to identify the measurement - collection of key/value pairs strings; 3) Field set: A set of values associated with the measurement - which can be int64, float64, bool or string; 4) Timestamp: When the last

measurement was taken.

The final task was to set up a dashboard in Grafana (<https://grafana.com/docs/grafana/latest/getting-started/get-started-grafana-influxdb/>) that will let us see the data that it is being added to the InfluxDB database. We will look at how to add one for the oscilloscope data and other variables from it, like mean, standard deviation, etc. A dashboard in Grafana is represented by a JSON object, like the influxDB, which stores metadata of its dashboard. Dashboard metadata includes dashboard properties, metadata from panels, template variables, panel queries, etc [15].

In order to do this, after the installation procedure, we have to open a web browser on the computer and open the Grafana dashboard by heading to `http://raspberrypi.local:<portnumber>` or `http://<hostname>:<portnumber>` or `http://<ipaddress>:<portnumber>`, replacing the IP address or hostname or port number for the actual setup.

2.18.2 Global System for Mobile Communication (GSM)

Phone calls relay signals from one place to another, like satellite communications or a television show. GSM is a digital cellular technology used for transmitting mobile voice and data services. GSM is a circuit-switched system that divides each 200 kHz channel into eight 25 kHz time-slots. GSM operates on the mobile communication bands 900 MHz and 1800 MHz in most parts of the world. In the US, GSM operates in the bands 850 MHz and 1900 MHz. GSM makes use of narrowband Time Division Multiple Access (TDMA) technique for transmitting signals. GSM was developed using digital technology. It has an ability to carry 64 kbps to 120 Mbps of data rates [25].

For this project we had the Waveshare SIM7600X 4G HAT, which allows Raspberry Pi to easily make a telephone call, send messages, connect to wireless Internet, global position, transfer data via Bluetooth, and so on [WaveShare]. The default relationship between SIM7600 control pins (the brainbox on top of the Waveshare 4G HAT) and Raspberry Pi IOs is shown in the table 2. This is important to know before attaching extra hardware to the GPIO Pins on the Raspberry Pi. It is good to know that this is not the only way to connect these devices. When the Pi is back up, the SIM7600G-H 4G Hat's PWR LED must be lit. Now press the PWRKEY button on the board — after a brief moment, the NET LED should be light up. We have connected GSM and Raspberry Pi as can be seen in 31.

In the device Waveshare SIM7600X 4G HAT in the front interface (lower right image in the Fig. 31) we have 1) PWR: power indicator; 2) NET: Network status indicator; 3) PWRKEY: power switch; 4) USB to UART interface: for serial debugging, or login to Raspberry Pi; 5) USB interface: for testing AT Commands, gettings GPS positioning data, etc; 6) 3.5 mm earphone/mic jack. In the back interface (upper right image in the Fig. 31) we have: 1) TF card slot: allows file/SMS/..storage; 2) SIM card slot: supports 1.8V/3V SIM card; 3) Raspberry Pi GPIO header: for connecting with Raspberry Pi.

Table 2. GPIO Pins Utilised by HAT

SIM7600	IO Raspberry pi 4B	Description
5V	5V	Power Supply
GND	GND	Ground
TXD	RXD	UART Pin
RXD	TXD	UART Pin
PWR	P22	Power up module
FLIGHTMODE	PC7	Flight mode

There must be a connection between PWR and D6.

**Figure 31.** Raspberry Pi and GSM [Nair] (*Rpi and GSM*)

To test this device, the following components were prepared: 1) SIM7600G-H 4G HAT(B) × 1 ; 2) LTE Antenna × 1; 3) USB-A to micro-B cable × 1.

The first attempt made was using the GPS of the GSM because we did not have a valid SIM card. Navigation satellites help us to find our way by beaming signals to GPS receivers on the ground. Although satellites communicate with the ground using antennas, the test was made without using the antennas of the device to the Raspberry with a python script following the code bellow.

```
wget https://www.waveshare.com/w/upload/2/29/SIM7600X-4G-HAT-Demo.7z
sudo apt-get install p7zip-full
7z x SIM7600X-4G-HAT-Demo.7z -r -o/home/pi
sudo chmod 777 -R /home/pi/SIM7600X-4G-HAT-Demo

cd /home/pi/SIM7600X-4G-HAT-Demo/Raspberry/c/
sudo ./sim7600_4G_hat_init
cd ..
```

Table 3. SIM7600X module supports AT command control. For more AT commands, please refer to: SIM7600X series AT command set

Command	Description
AT	AT Test Command
ATE	ATE1 set echo, ATE0 close echo
AT+CPIN?	Read PIN
AT+CGMI	Request manufacturer identification
AT+CGSN	Request product serial number identification
AT+CSUB	Request product version - Flight mode
AT+IPREX	Configure baud rate of model
AT+CSQ	Query signal quality
AT+CREG?	ME network registration status
AT+CPSI?	UE system information
AT+CGREG	Set default value for GPRS network registration status
AT+CGREG=1	enable network registration unsolicited result code

```
cd Gps
sudo make clean           //Clear the original execution file
sudo make                  //recompile
sudo ./GPS                 //Run the program
```

2.18.3 Raspberry Pi networked with GSM

The GSM has a bidirectional communication between the server and client using AT commands for that. AT Commands can be used to test a modem or other communications device to see if it is working properly. They can also be used to configure a modem or other communication devices.

It is possible to use a serial terminal like “minicom” to start communicating with the modem and check if it is working well. Minicom is a terminal emulator program. The code to communicate SIM7600x Module by minicom at the command line or in a desktop Terminal run:

```
ls /dev/ttyUSB2
sudo minicom -D /dev/ttyUSB2
AT+CUSBPIDSWITCH=9011,1,1
AT+CUSBPIDSWITCH=9001,1,1
```

The port used was the USB2 port. The GSM modem had a baudrate of 115200. It is important to guarantee that there is no PIN in the SIMCARD, it is possible to deactivate in a private phone. The PIN from the SIM card on the phone was deactivated and then, it was possible to see the information about it. Some basic AT commands are shown in the table 3. Another option would be python library. There are also wraps AT command errors into Python exceptions in the gsmodem python library (<https://pypi.org/project/python-gsmodem-new/>).

After testing and verifying that the SIM card has a valid internet connection, it is necessary to have a connection to the SIM card. This is not automatically done by the Raspberry Pi (<https://www.twilio.com/docs/iot/supersim/getting-started-super-sim-raspberry-pi-waveshare-4g-hat#hardware-setup-the-sim7600g-h-4g-hat>) Some commands regarding the installation via terminal has been done:

```
ifconfig
sudo dhclient -v usb0

ifconfig -a
sudo apt install raspberrypi-kernel-headers
sudo apt-get install --reinstall raspberrypi-bootloader raspberrypi-kernel
sudo su
make clean
make
ls
insmod simcom_wwan.ko
lsmod

sudo su
rmmod qmi_wwan
wget https://www.waveshare.com/w/upload/0/00/SIM7600_NDIS.7z
sudo apt-get install p7zip-full -y
7z x SIM7600_NDIS.7z -r -o./SIM7600_NDIS
cd SIM7600_NDIS
```

After that, some steps that will be shown below: 1) Open the wwan0 interface; 2) Send by AT command; 3) Assign the IP address; 4) Then it is possible to try to ping a website for a try. It is important to always verify if there is a valid IP address. If there is dns error, the following command can fix it: "route add -net 0.0.0.0 wwan0". To test all these topic:

```
ifconfig -a
sudo ifconfig wwan0 up
minicom -D /dev/ttyUSB2
AT$$QCRMCA=1,1
apt-get install udhcpc
udhcpc -i wwan0
ifconfig -a
ping -I wwan0 www.waveshare.com
route add -net 0.0.0.0 wwan0
```

Point-to-Point Protocol (PPP) is a TCP/IP protocol that is used to connect two computer systems. Computers use PPP to communicate over the telephone network or the Internet. PPP connections are made through a physical connection, such as a telephone line or the Internet. PPP allows for data transfer between the two systems, as well as interoperability between different manufacturers' remote access software. PPP also allows multiple network communication protocols to use the same physical communication line [IBM].

Moreover, PPP is a Layer 2 protocol, which means that it uses the data link layer of the OSI model. PPP is a reliable protocol that has been around for many years. It is a relatively simple protocol, but it is very effective. PPP supports a full-duplex connection, such as Ethernet or point-to-point links. Once the link is established, data can be exchanged between the two nodes using the network-layer protocols that have been configured. PPP also includes mechanisms for error detection and correction, as well as for flow control to ensure that the data is transmitted smoothly.

To use a Raspberry Pi with a modem, the PPP is a good way to do a point-to-point connection. PPP is most commonly used to establish a connection between a computer and a modem, but it can also be used to connect two routers or two computers. In order to do this, we follow the following steps:

```
ifconfig -a  
sudo apt install ppp  
cd /etc/ppp  
sudo pon  
ip a  
route  
ping -I ppp0 8.8.8.8  
curl --interface ppp0 8.8.8.8  
sudo route add -net "0.0.0.0" ppp0  
route
```

Now, the final shell script must always initialize the service pon as bellow:

```
sudo pon &  
sleep 15  
sudo route add -net "0.0.0.0" ppp0
```

2.18.4 Tunneling

Tunneling is the process of encapsulating data from one network protocol within packets used by another network protocol. This allows network traffic designed for one network to be sent through a different network.

In computer networks, tunneling is often used to encapsulate one communication protocol within

another.Tunneling is often used to allow private network communications to be sent through a public network, such as the Internet.This allows a network to carry a protocol that it does not support natively [ngrok community].

If the tunnel status is “online” it is possible to open the Raspberry Pi terminal using Putty anywhere. The Host Address and the Port Number is shown in the picture below; it is used to access the Raspberry Pi.

Ngrok HTTP tunnels allow you to route HTTP protocols quickly and easily. These include websites, RESTful APIs, web servers, websockets, and much more. To use ngrok, you must have an account. To register a new account, visit the sign up page. You can also use a Google or GitHub account for easy signup.

Starting an HTTP tunnel is an easy way as typing ngrok http 80, or other local port that the service is running on. For a full list of options for starting HTTP tunnels, see our ngrok agent HTTP Tunnel reference. To activate grafana in the http ngrok:

```
ngrok http 3000
```

For the Raspberry Pi operating systems we support, their default file locations are:

Linux: `"~/config/ngrok/ngrok.yml"`

The most common use of the configuration file is to define tunnel configurations. Defining tunnel configurations is useful because you may then start pre-configured tunnels by name from the command line without remembering all of the right arguments every time. It is also possible to use this method to start more than one tunnel from a single ngrok agent. Tunnels are defined as mapping of name into the configuration under the tunnels property in the configuration file. The following code defines two tunnel.

```
authtoken: authtoken created
tunnels:
  first:
    addr: 50001
    proto: http
    hostname: in.free.plan.there.is.no.hostname.com
    hostheader: in.free.plan.there.is.no.hostname.com
  second:
    addr: 50002
    proto: http
    hostname: in.free.plan.there.is.no.hostname.com
    hostheader: second-in.free.plan.there.is.no.hostname.com
```

We have used the http to visualize grafana and tcp to enter the Raspberry Pi terminal. It is possible verify what has been shown in the Raspberry in the Fig. 32 and 33.

```
ngrok
Hello World! https://ngrok.com/next-generation

Session Status          online
Account                 Mônica Emediato (Plan: Free)
Version                3.0.4
Region                 Europe (eu)
Latency                25ms
Web Interface          http://127.0.0.1:4040
Forwarding             tcp://2.tcp.eu.ngrok.io:13936 -> localhost:22

Connections            ttl     opn      rtl      rt5      p50      p90
                        0        1        0.00    0.00    0.00    0.00
```

Figure 32. Ngrok configuration 1 tunnel (*1 tunnel*)

```
ngrok
Hello World! https://ngrok.com/next-generation

Session Status          online
Account                 Mônica Emediato (Plan: Free)
Version                3.0.4
Region                 Europe (eu)
Latency                22ms
Web Interface          http://127.0.0.1:4040
Forwarding             https://lf87-92-110-108-4.eu.ngrok.io -> http://localhost:3000
Forwarding             tcp://5.tcp.eu.ngrok.io:14865 -> localhost:22

Connections            ttl     opn      rtl      rt5      p50      p90
                        0        0        0.00    0.00    0.00    0.00
```

Figure 33. Ngrok configuration 2 tunnels (*2 tunnel*)

Finally, we want to connect to the TiePie Oscilloscope first, do measurements and collect data. Secondly, we would like to connect to the Internet with GSM and send information through InfluxDB and visualize it in Grafana. After that, we would like to verify the hosts open through Ngrok as previously showed. In order to have the tunnels running we can create shell files.

To do this, in the Unix terminal on the Raspberry Pi we created scripts files with .sh extension and it was set an execute permission on the script using chmod command. The orchestration for all the implementations was done through shell scripts and crontab commands to perform in specific times every day.

Besides that, some instabilities were seen to initialize the influxdb and in the ppp protocol in the Raspberry Pi using pon. It is necessary to read the documentation about the influxdb because there are versions problems not fixed. It is important to verify the file "sudo nano /etc/ppp/peers/provider" if the protocol PPP is not working in the Raspberry Pi. The following code proved to be enough to establish the connection and verify the APN name. There are multiple ways of configuration of the APN, via AT Commands or via Phone are two possibilities of many ones.

```
/dev/ttyUSB2
connect '/usr/sbin/chat -s -v -f /etc/chatscripts/gprs -T [APN_NAME_CAN_CHANGE_ANYTIME] '
```

```
nocrtscts
debug
nodetach
ipcp-accept-local
ipcp-accept-remote
```

2.19 Chapter Summary

The chapter can be summarized as an insight into the materials, setup, measurement protocol and the signal processing techniques that we have used to implement the project and fulfill the objectives.

In this work the authors built a setup, using modern measurement instruments in combination with available processing power, to create a system which allows real-time control of equipment, as well as logging and processing electric current data of different ES modes.

During this chapter there is a open question that this work aims to answer: "What is relevant for your application?". We need to be aware and make decisions concerning the setup design, mainly the liquid (volatility, solvent properties, viscosity, surface tension), illumination (optical access to the spray-mode: cone, spray, jet break up), current transport (safety, impedance matching/self stabilization). There is not only one correct answer and this will change for every application.

The focus is to further extend the ES mode current classification proposed [28], but also to explore streaming/corona signals and verify whether such current data can be used to prevent discharges. Additionally, more advanced signal treatment techniques are used and tested to verify whether other variables can be included in the current classification as mention in this chapter.

The method presented in Chapter 2 have included a description of the research design, the sample size, the data collection methods, and the data analysis methods. The heart of the setup is a purpose-made Python library which is used to remotely control the power supply and the syringe pump, as well as to acquire and process the data collected by the oscilloscope. Data is acquired in sampling blocks of 500 ms, using 50 k sample points at a sampling rate of 100 kSps. For each block the mean, RMS, standard deviation, and FFT are calculated. The results are further used for automatic classification of this signals representing the currents of the spray. First classification attempts were based on previous work [28]. Furthermore, all data points are stored in JSON format along with liquid and setup data. The stored data can be used for offline processing to confirm existing relationships between quantities like e.g. current and flow rate [4, 10, 18] and to generate meaningful diagrams based on, if necessary, a vast amount of data measurements. The Python program correlates the treated values of the electric current with a specific voltage and different plots can be generated relating the current values with a specific potential window. This means that

the developed Python library allows remote control of the power supply and pump, as well as to acquire and process the measurement data from the oscilloscope.

Using the variables proposed by Verdoold et al. (2014), the program checks the electric current values and automatically identify which mode is running at a certain voltage-flow rate window.

3 Results and discussion

In this chapter we present the obtained results. From this project the main outcomes are:

- Software development;
- Co-routines to control the entire setup were designed;
- Digital signal and statistics techniques for spray-modes classification;
- Logging the information in a viewer window (offline visualization);
- Predict discharges (knowledge of the region before it happens);
- Automated system: prospective automation of the EHDA process;
- Datalogger with Raspberry Pi and GSM for monitoring the EHDA system;

Different insights on how to accomplish the results were found. These insights were obtained from the different activities carried out and are thus divided into two categories: ES-modes Classification and Spark Suppression.

Initially, JSON files were generated for each class as shown in Figure 34.

```
> {} setup6ethyleneglycolcone_jet6769.0V6.11116e-13m3_s.json > ..
{
  "config": { ... },
  "processing": [ ... ],
  "measurements": [ ... ]
}
```

Figure 34. JSON file example

Inside the fields, the code bellow shows how the JSON files are after software development. The method previously in Chapter 2, subsection 2.8 showed how the division of variables would be. This can be seen in this code automatically made by the SmartSpark with real values from the oscilloscope.

```
{
  "config": {
    "liquid": {
      "name": "ethanol pure",
      "surface tension": 0.0219,
      "dielectric const": 24.55,
      "viscosity": 0.001086,
```

```

"density": 784.93,
"electrical conductivity": 0.00378,
"unit system": "SI",
"vacuum permitivity": 8.85e-12,
"slope chen pui": 10.0,
"flow rate min": 6.532277976865393e-14 },
"setup": {
    "syringe color": "brown",
    "camera to nozzle distance": 16.5,
    "config": "nozzle to plate",
    "nozzle to plate or ring distance": 2.0,
    "syringe diameter": 0.136,
    "syringe outside": 0.165,
    "syringe height": 3.5,
    "high voltage": "HV on the nozzle",
    "diameter syringe": 0.16,
    "units": "cm",
    "coflow gas type": "none",
    "voltage regime": { "sequency": "ramp",
        "start": "3000",
        "stop": "12000",
        "slope": "100",
        "size": "0",
        "step time": "3" },
    "comments": "" } },
"processing": [ {
    "mean": -2.3827574253082275,
    "variance": 18.79721450805664,
    "deviation": 4.335575580596924,
    "median": -2.51572322845459,
    "rms": 4.947195529937744,
    "psd welch": [...],
    "fourier peaks": [ "1st: ", [119137.86164909601, 0.0],
        "2nd: ", [39668.39053313087, 50.0] ,
        "3rd: ", [2999.64243738513, 100.0] ] ],
"measurements": {
    "data [nA)": [...],
    "flow rate [m3/s)": 2.7778e-10,
    "voltage": 3042.7,
    "current PS": -3.76554e-07,
    "temperature": 21,
}

```

```

"humidity": 31,
"date and time": "Thu_31 Mar 2022",
"spray mode": { "Sjaak": "dripping",
    "Monica": "no streamer onset" }} }

```

Even though the tests were conducted with defined sample rates and different voltage regimes (step, ramp), the proposed setup was enough to detect the spray-modes and know the pre-spark region in the range which is most applicable for this kind of application. This was only done because the system was automated via oscilloscope, pump and HVPS.

The HVPS works with DC and the SmartSpark is AC, so, it is not possible to use the electric current data from it. We can see this in the Fig. 35 when we collected electric current data from the HVPS there are small random numbers. The data from the power supply is only used in relation to the real-time voltage and the measurements.

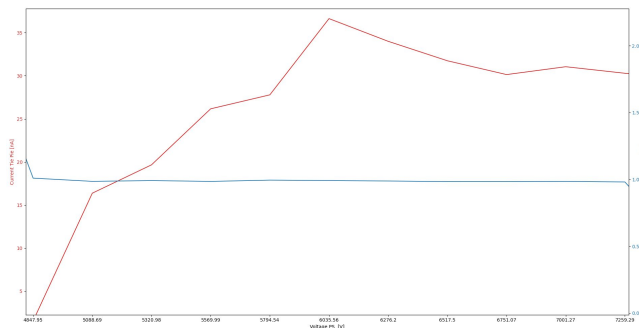


Figure 35. Red as Current TiePie versus blue Current HVPS

The results of the different setups will now be presented. 1) Tests performed with the oscilloscope on the High Voltage side showed that the signal is noisier than only in the ground line. This can be caused by a number of reasons, including electrical interference, bad wiring or soldering, larger wires, the wiring was done without fittings cables or even distance. The further away the signal is from its source, the more likely it is to be interfered with because there is an antenna effect. The HVPS works by amplifying an input voltage and it is possible that it amplifies the noise coming from the electricity network. But, we can still verify the shape of each classification of ES. 2) Parallel capacitor made no difference in the setup.

In relation to the ring setup (see Figure 13), it is better to apply the high voltage on the ring as well, for example. Liquid accumulation due to droplet flyback was seen in the ring (see Figure 36).

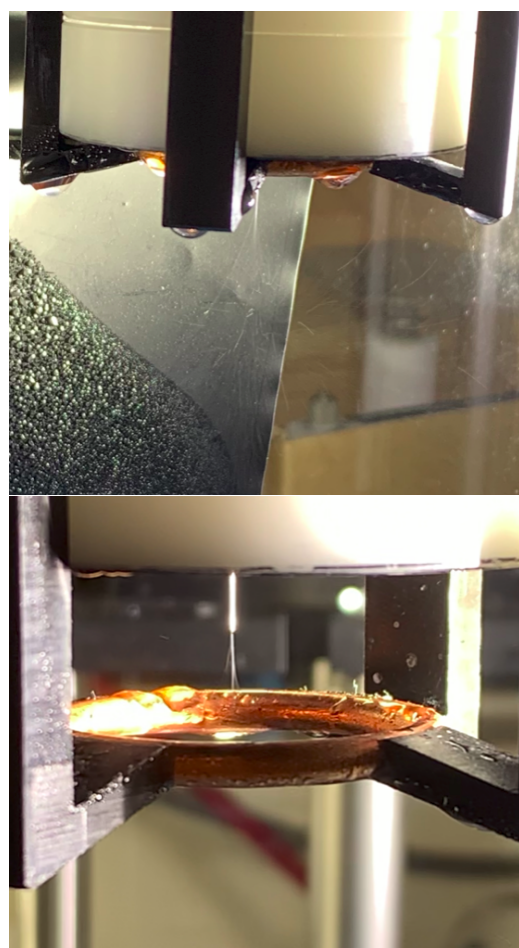


Figure 36. Wet ring setup

3.1 Electrospray Modes Classification

3.1.1 Non-automatic Control as First Approach

In order to do the classification, the Measurement Procedure described in section 2.10 shall be able to facilitate that the following procedures are similar and that there is a standard to be followed. Furthermore, the oscilloscope images (see figure 37) show different electric current signals, measured by the oscilloscope, for different conditions. It can be observed that the shapes of the signals are different for each ES mode and quite similar to those reported by Verdoold et al. (2014).

Moreover, the obtained signal shape of the electric current was matched with the spray-mode using the high speed images (see figure 38). In addition, the high speed allows good monitoring and measurements.

The code does print screens from the high speed camera. Finally, it is possible to generalize that in the section 2.6 proved to be a good start to validate our system although there was no automation involved.

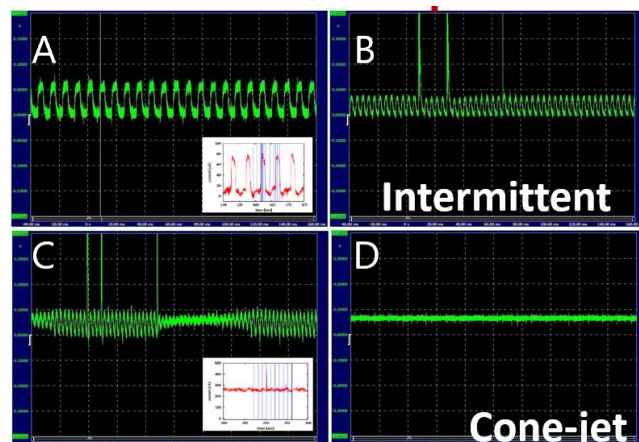


Figure 37. Working conditions: Flow rate: 2 μ L; a) Fast dripping: 3642 V; b) Intermittent: 4464 V; c) Transition Intermittent to cone-jet: 4674V; d) Cone-jet: 4860 V. Printscrean of spray-modes from the oscilloscope TiePie

Under the experimental conditions different ES modes were observed using a constant flow rate while increasing the applied voltage manually. Some of this difference can be seen in the magnetic and shape of the EHDA signal of the electric current and also visually in the liquid jet that is surrounded by an electrical field. A number of experiments were performed at the oscilloscope at sample rates of 20 kHz and the time interval of measurement of 5×10^{-5} s (Table 3).

The nozzle used was an EFD precision with ID = 0.41 mm, OD = 0.75 mm (blue nozzle). The high voltage (FUG HV power supplies) was applied to the nozzle while keeping the counter electrode grounded. The validation of the obtained electric current values (in the cone-jet mode) was done by comparing the values obtained by Chen and Pui et al. (1997) [4]. We can see in the table that the results show the linearity addressed in the literature. Validation proves that we are on the right path.

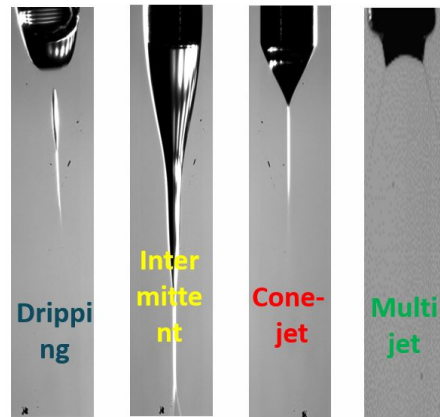


Figure 38. High speed camera images of the High Voltage Lab for Ethanol. Fps: 12500, shutter speed: 1/950000, Flow rate: 2 μ L/a) Dripping: 3032 V; b) Intermittent: 4464 V; c) Cone-jet: 4860 V; d) Multi-jet: 6052 V.

Table 4. Electric current values in the Cone-Jet mode. R = 1 M Ω and measurement instrument uncertainties for Ethylene Glycol

Flow rate [ml/h] (± 0.01)	Voltage [kV] (± 0.005)	Current [nA] (± 0.0005)
0.10	4.928	17.3400
0.20	5.226	22.8700
0.30	5.226	28.8600
0.40	6.366	28.8900
0.50	6.366	29.8900
0.60	6.366	34.1400
0.70	6.366	37.5500
0.80	6.366	38.3200
0.90	6.366	41.7400
1.00	6.366	44.1000
2.50	5.957	48.3000
5.00	5.945	77.5100

3.1.2 Automatic Approach

The implementation of an automatic classification of the ES modes was initially based on the same statistics proposed by [28]. The electric current mean is gonna be referred as "VAR0". The Relative standard deviation of electrical current divided by mean its is gonna be referred as "VAR1". The mean divided by median will be "VAR2". After the collection of data with JSON, a viewer to analyse each mode was done. It is possible to verify in the Figure 39 the similarities of the signal based on Verdoold et al. (2014).

After that, it was possibly to compare the variables involved in the system. Moreover, more diagrams were built in order to see the best way to analyse the signal. In the figure 40 is possible to see three different liquids. The box plot is comparatively short. This suggest that overall data have a high level of agreement with each other. For continuous spray there is no pulse pattern visible, but minor fluctuations.

The literature helped but the present work extended what has been done. New features were added and improvements were made such as including statistics of FT coefficients of the signals. This was possible by visualizing all ES-mode in a methodical and automated way. Moreover, it is possible to say that the low pass filter proved to be enough to have good conditions to use the FT. In addition, FT proved to be a important classifier in the ES system. We could see there is no dominant peak in the cone-jet mode and when we have a stable EHDA system.

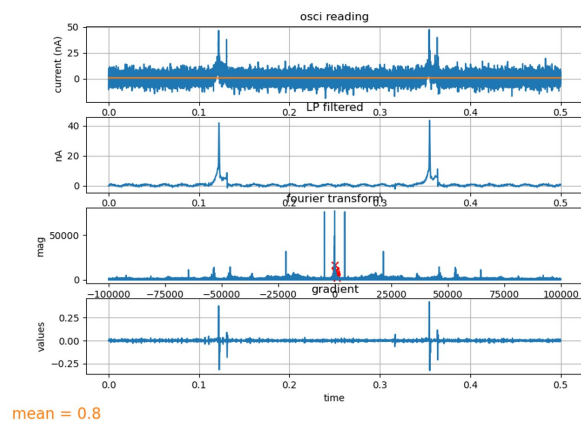
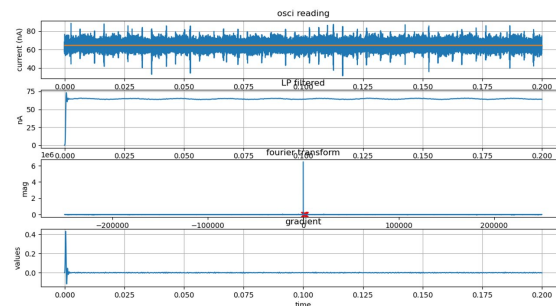
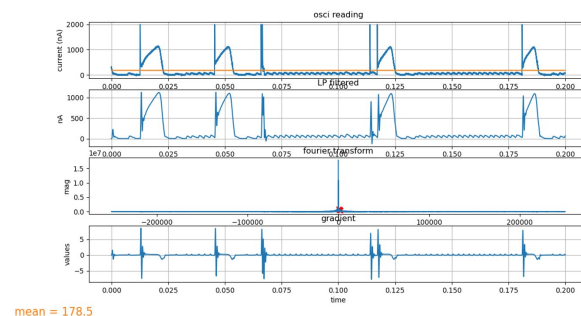
There is a region in the FFT of no interest, since it is part of the DC component and part of the electrical system (up to 50 Hz). 50 Hz notch filter (removing fourier coefficients at 50 Hz and calculating inverse FFT) was implemented.

Since the FT needs to use a pattern, we could see this for the ES-modes. There is a FT peaks transformation for every shape - specially for multi-jet 39c, where we could verify that in greater flow rates, we have more peaks than in a smaller flow rate. In the intermittent mode was possible to see an annoying high pitch is going to show up just as a spike at some high frequency. The power spectrum shows the range of the dominant frequencies. High pass filter is not necessary.

After the automatic classification of the code, the signal histogram diagram for each mode was made. Based on a vast amount of data, we have a histogram made with the JSON files generated by the SmartSpark. Histogram and Gaussian of the parameters help the visualization of the current data because we can see the distribution of the current for each spray-model in the Fig. 41. For each spray-mode we have different current ranges. Until the system go to the current ranges from a few nA up to greater than 1 μ A (already SC, partial discharges) but always smaller than 3 μ A.

It is also possible to relate mode of the camera with the current. This can be done via synchronization with the measurements and the prints screen (already implemented).

The constant characteristic of the cone-jet mode makes the spark detection and prevention de-

(a) Dripping signal (*User offline dripping signal*)(b) Cone-jet signal (*User offline window cone-jet*)(c) Multi-jet signal (*User offline multi-jet signal*)**Figure 39.** Offline Viewer

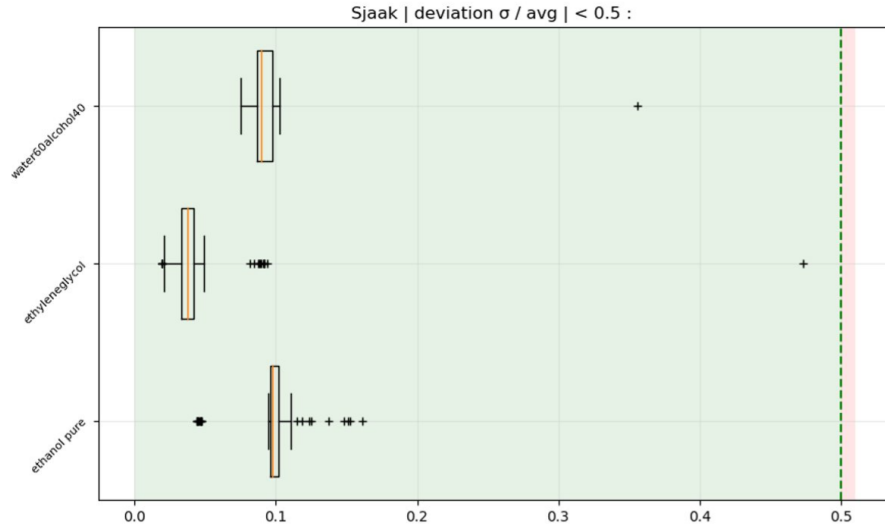
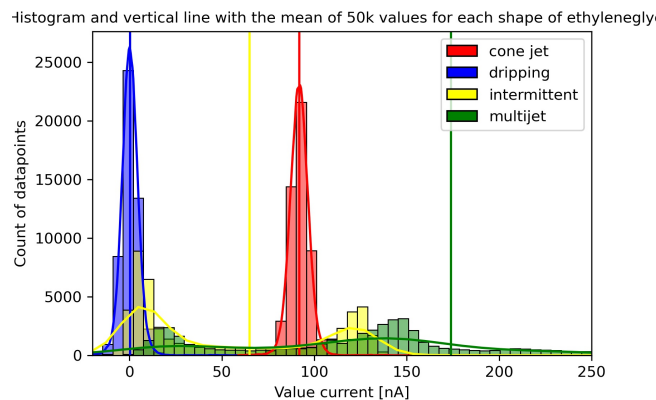
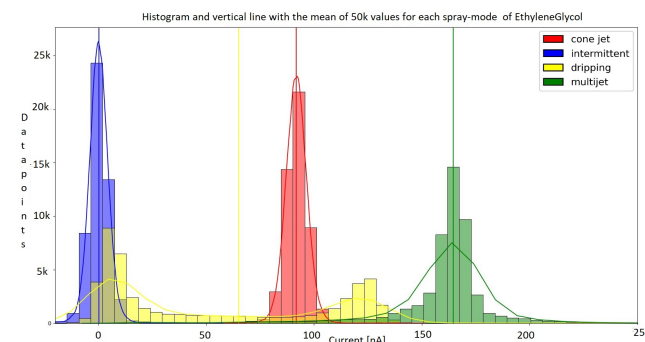


Figure 40. Box plot for different liquids for the standar deviation divided by mean for cone-jet based on the values proposed by [28]



(a) Unstable histogram



(b) Stable histogram

Figure 41. Histograms generated by SmartSpark

velopment possible and essential to predict the peaks of current and voltage in the system. The scenario of peaks can be very dangerous in industrial environmental. It is possible to predict value based on previous data. There is a model for each classification mode. It is necessary to bring experimental and different variables and conditions in the setup to provide a setup that can be used in real life applications in a general way.

Diagrams were created in order to compare the variables and improve the classification of the system. This can be seen in Fig. 44, 45 and 42 and they are in the Ramp mode with the following specifications: "start": "3000" [V], "stop": "11000" [V], "slope": "200" [V/s].

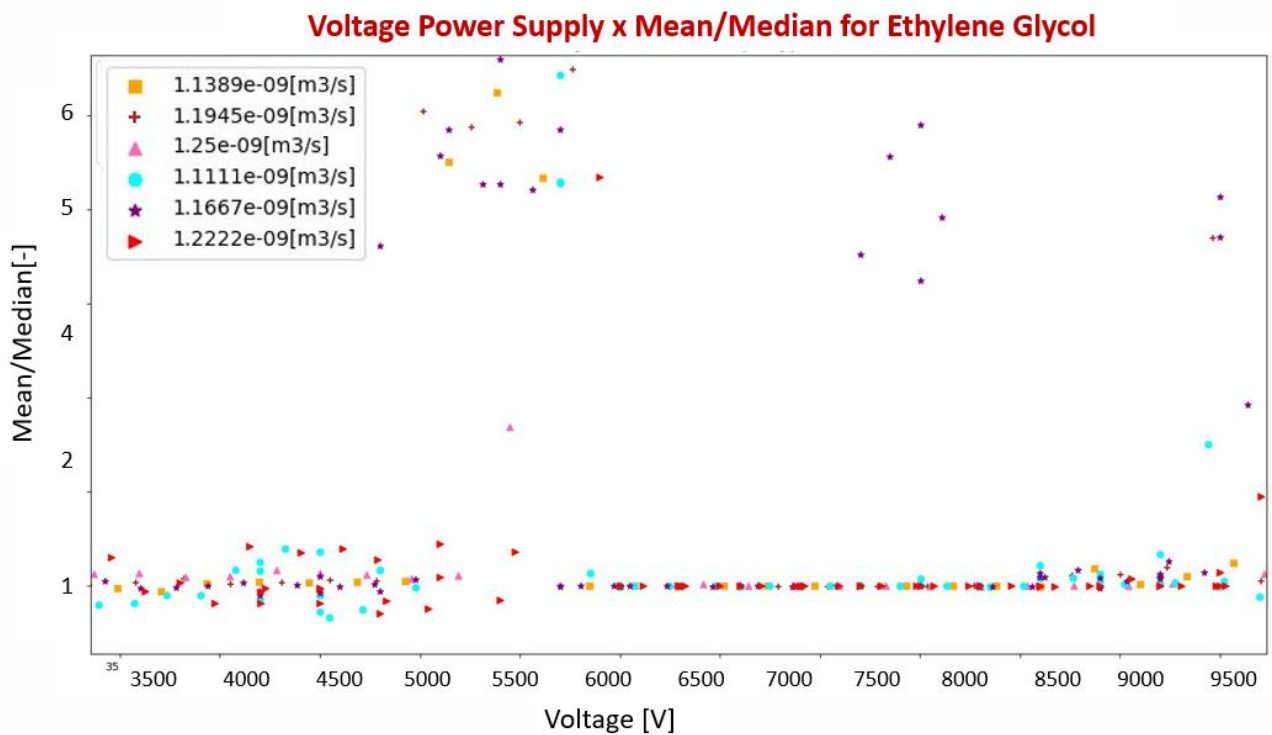


Figure 42. VAR2 for Ethylene Glycol (*Nozzle diagram*)

The step mode is not good for show the characteristic of the system. In the step mode there is "start": "3000" [V], "stop": "11000" [V], "slope": "350" [V/s], "size": "300" [V], "step time": 5 [s]. See figure 47

Based on that, we could verify the voltage and current window for different flow rates.

3.2 Spark Suppression

The frequency of the spark peaks are well defined based on the flow rate, voltage regime, current region, setup geometry and liquid properties. Although, if we know the region after the spray-mode multi-jet window, we can prevent sparks.

Streamer corona (SC) is the region where the sparks begin. SC signal can be seen in the picture 49 below. It is possible to say that there is no discharge without SC. A significantly jump in the mean

3.2 Spark Suppression

3 Results and discussion

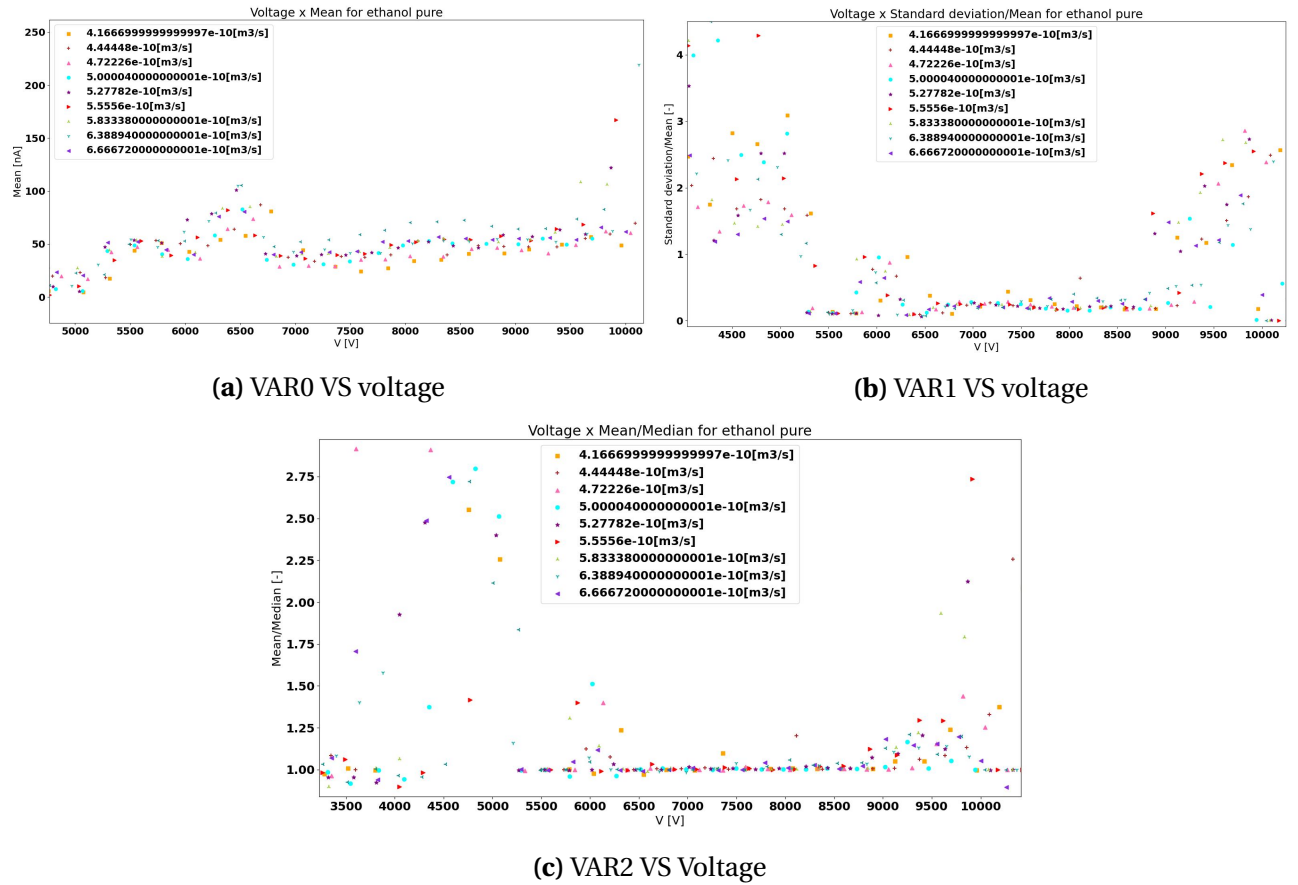


Figure 43. Smart Spark processing results for a configuration as the diagram of Figure 11; system spraying ethanol.

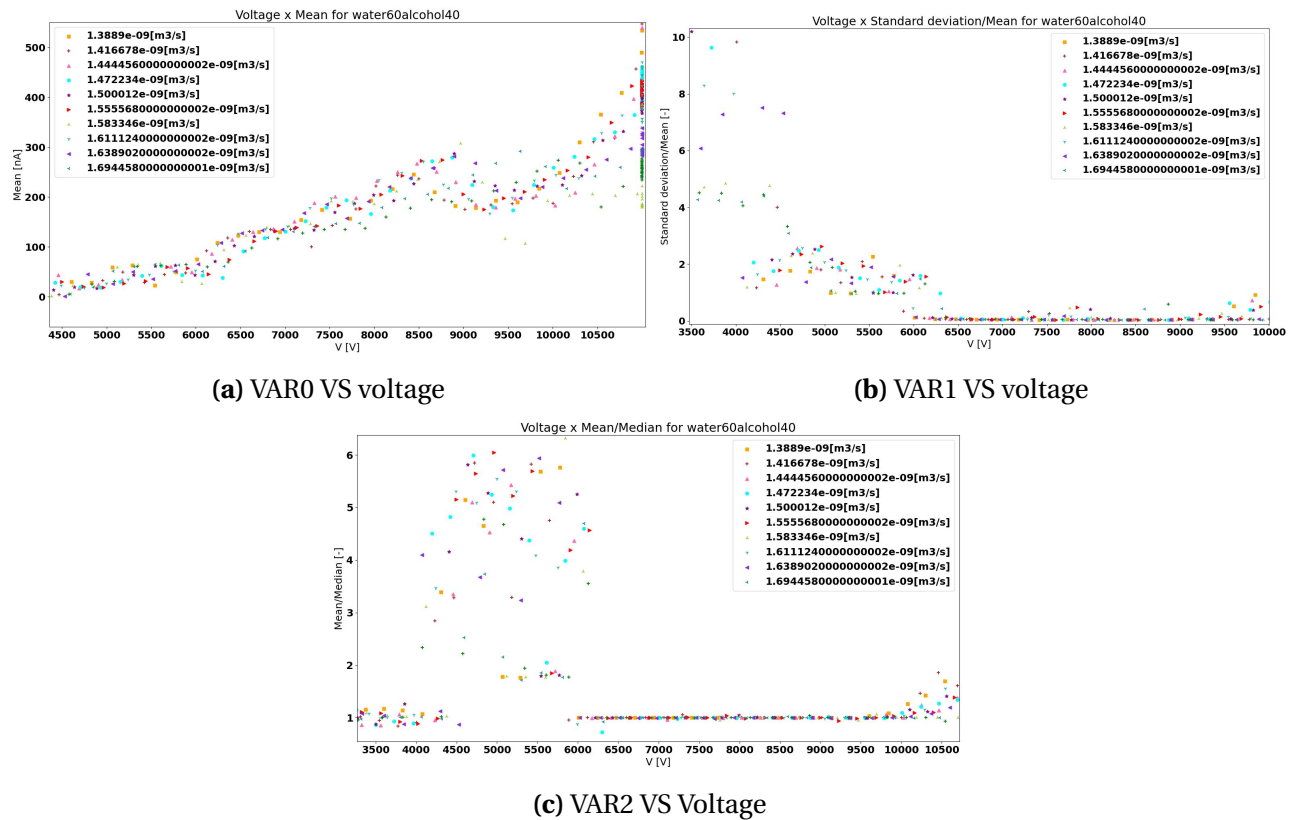


Figure 44. Smart Spark processing results for a configuration as the diagram of Figure 11; system spraying wateralcohol.

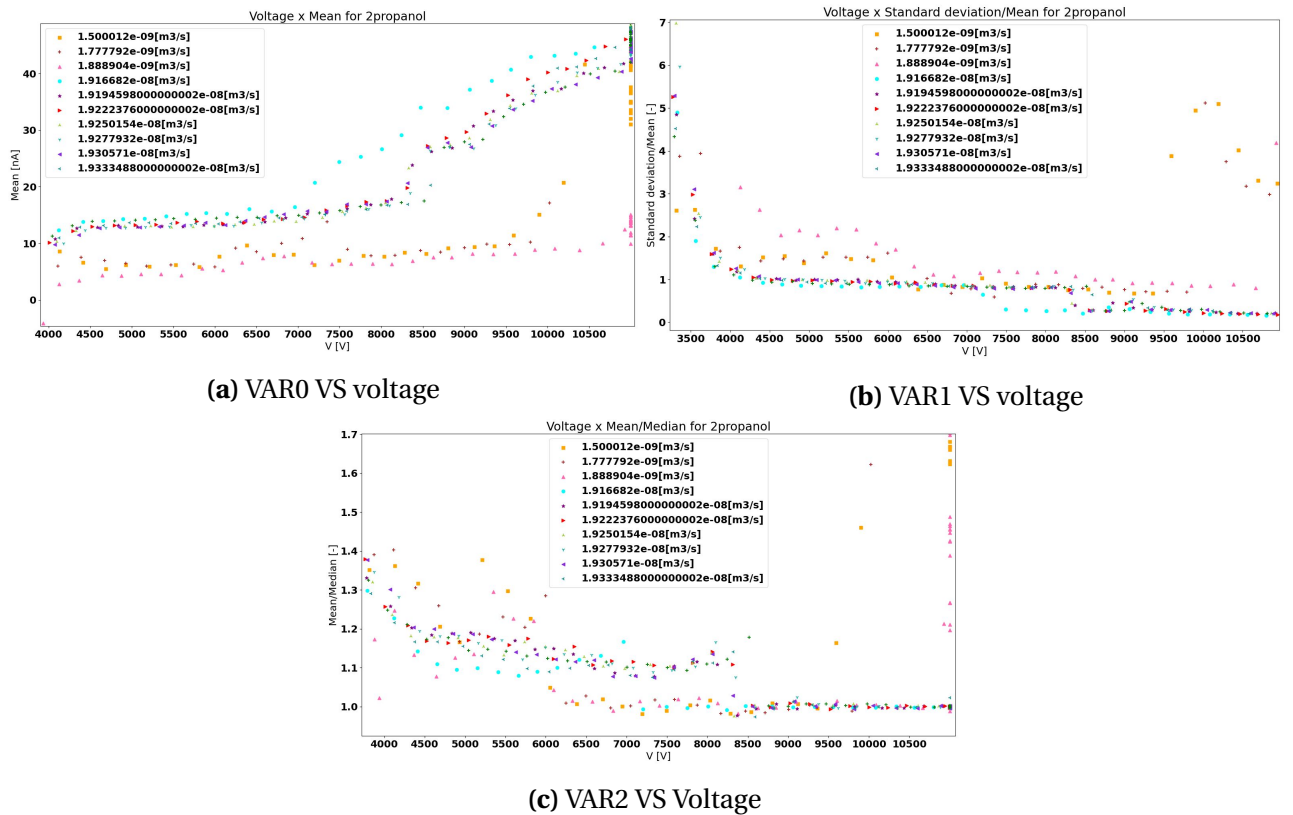


Figure 45. Smart Spark processing results for a configuration as the diagram of Figure 11; system spraying 2propanol.

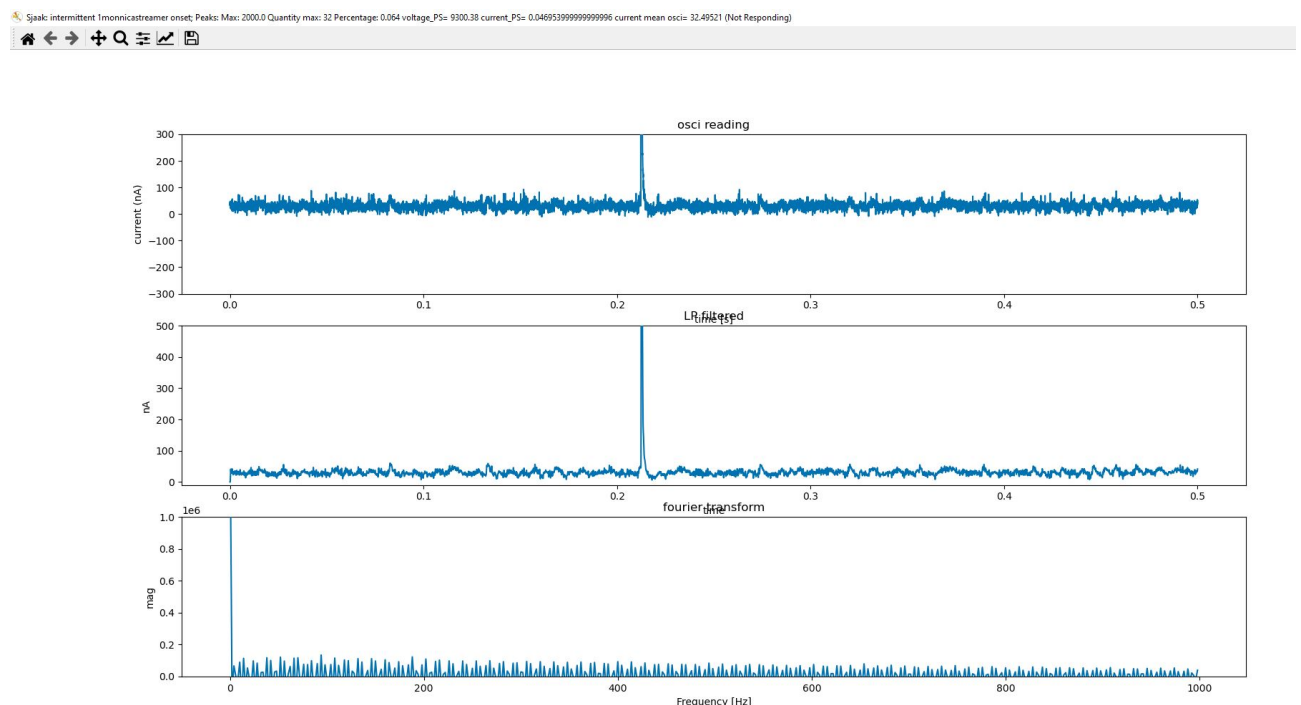


Figure 46. The classification can be seen in the window on the left and counts on the classification made by Sjaak et al. (2014) (*User main window*)

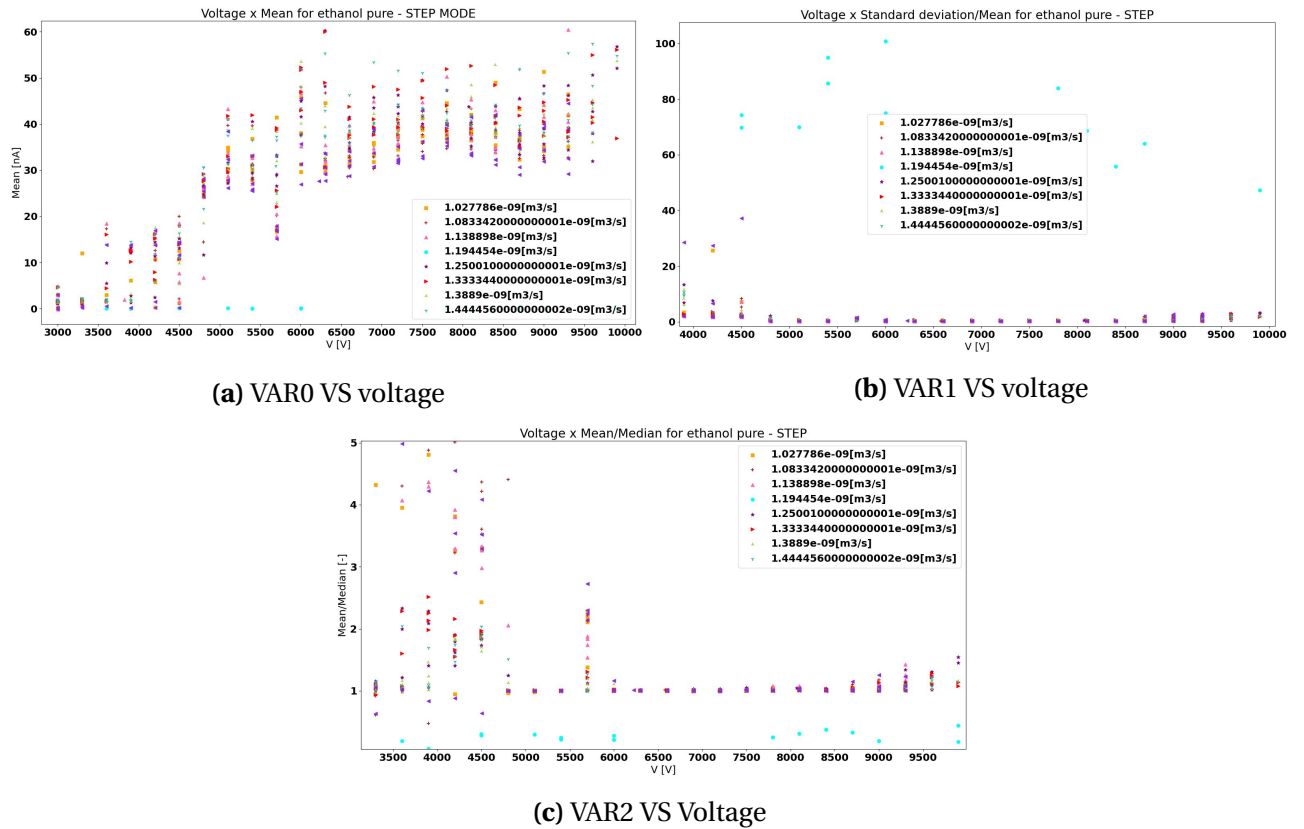


Figure 47. Smart Spark processing results for a configuration as the diagram of Figure 11; system spraying ETHANOL.

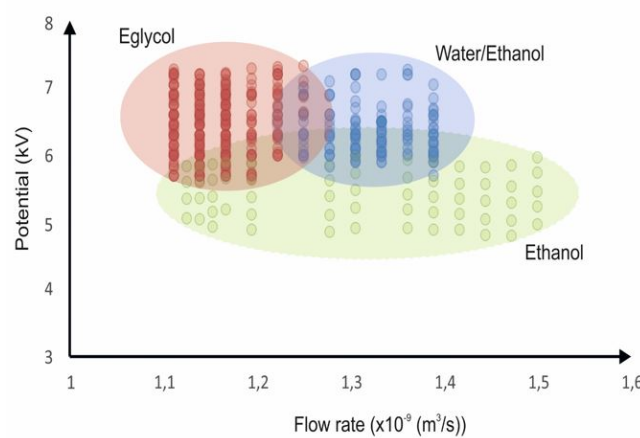


Figure 48. Operational window

value of the current indicates corona onset. This project consider the identification of the SC as an important region of the SmartSpark.

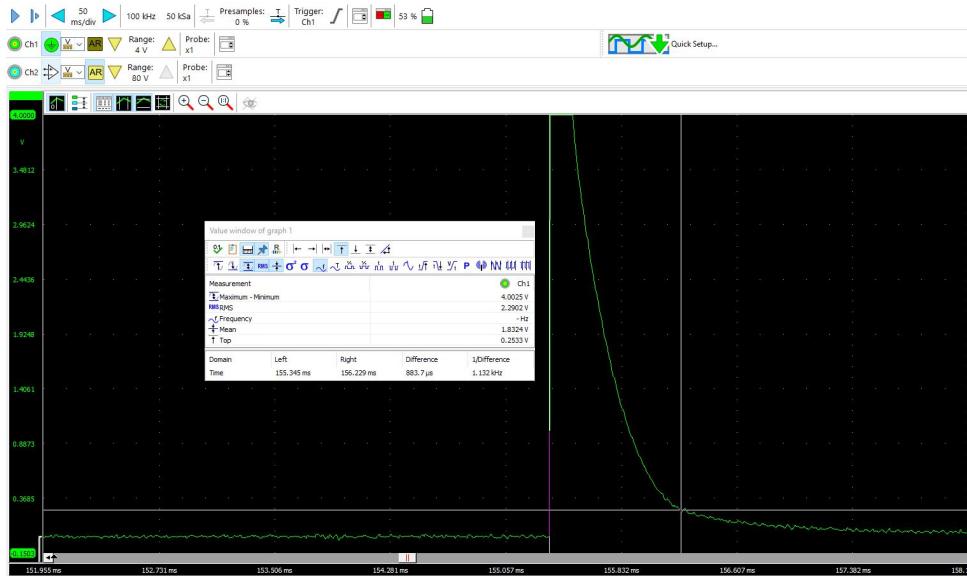


Figure 49. TiePie prinscreen signal of corona peak when $\alpha < 0$, i.e., α is negative, then the signal $x(t)$ is a decaying an exponential signal. (*Spark signal example*)

Based on a vast amount of data we could build a system that detect the region of multi-jet and also the region right after the multi-jet region, and we define it as pre-spark region or corona streamer onset in our classification method.

The spark suppression uses serial commands for shut down the power supply voltage, which can goes from 10 kV to 0 V in less than 2 seconds. For our setup, this time is sufficient. The generalization of the spark event and at what current level corona actually occurs depends on the setup and of the liquid properties. The pre-spark region can be seen as the main relay and comparative area in the operation and prevention of spark. We demonstrate a continuous process for the effective prevention of sparks reducing their charge in the multi-jet region using serial commands from the controller.

Obviously detecting plasma forming and reducing the voltage over nozzle to counter electrode proved to be enough with the Python code. This was done with dry setup, which means, no liquid and/or no flow rate while the voltage was increased until more or less 20 kV.

4 Conclusions

When looking back at the goal of automation of the EHDA process, it can be said that this was reached. Based on that, results have shown that the SmartSpark system can be used to measure the current and prevent discharges in ES applications because of the automation of the process. Such conclusion also implies that the proposed technology is also promising for different applications

in water technology, e.g. particle shape and density in reactors, annamox, etc, as well as for other industries, e.g. food technology, mining, etc.

The direct measurement with the oscilloscope TiePie WS6 DIFF of down to 10 nA is visible. The configuration chosen with a WiFi scope was proven adequate to transmit the signals without interference the measured data. In addition, it improved safety. Furthermore, we could confirm in this work that sample rates of 50 kS kilo for getting a signal from sparks is sufficient thanks to the integration with the Oscilloscope.

The physical setup, measurement devices used and the developed Python libraries for signal processing are sufficiently capable for real-time classification of cone-jet, intermittent, dripping, and corona streamer onset correctly. This was only possible thanks to the automation involved in the process.

SmartSpark is seen as an important tool towards the industrialization of EHDA processes. The compatibility between the bench scale tests and the real scale test have shown that, the technology will be used in real scale as showed in the GasUnie Implementation in chapter 2.18.

Choosing JSON as the desired format was driven by easy human readability over storage efficiency. A viewer class allowed visually browsing through 50 kS blocks and manually adjusting classifications. Regarding to the code, it was possible to acquire much knowledge about threads and serial control between two different systems and peripherals, as well as the use of the necessary conditions to have efficient resource consumption in a real-time application.

Besides, the execution of the work allowed us to visualize the difficulties when increasing the number of threads so that there is synchrony between the conditions and the variables and instruments that are made for control and reference checking.

Furthermore, we have conducted experiments with the ring configuration and the liquid particles were not going to the plate anymore and they were accumulating in the ring (see Figure 36). This is not a good situation and to avoid droplet flyback towards the ring we should change the setup. The test with the ring setup has also shown a limitation for higher flow rates than 100 $\mu\text{L}/\text{hr}$. It is, nevertheless, believed that such limitation can be easily overcome by exploring other configurations like small reflection distance, more power.

We can say that there are positive results when using the input resistor of the oscilloscopes directly as the shunt resistor. The oscilloscope has an internal input and we used as a shunt resistor and it helped minimize noise in the measurement. All the results were done based on the $2 \text{ M}\Omega$ default input resistance when is the differentiate mode.

In addition, we have extended the worked based on digital signal processing techniques and more accurate statistics variables, we have decreased the range of the statistics for the spray-mode cone-jet and we have added our own method for all the spray-modes and in the pre-spark region. Finally, we analysed results and we found out that the signal follows the expected behavior as previous

mentioned [28].

Electrospraying in nozzle-to-plate configuration allows us to stabilize the spraying process independently without the presence of High Speed Camera, only using the current values. Meanwhile, the high voltage setup configuration controlled mainly by the voltage difference between the ring electrode is sufficient.

Even though extended tests have to be conducted to verify the durability of the communication between Raspberry Pi and GSM module, it is possible to say that the data-logger of the current works. Nevertheless, long time test at low temperatures has to be done as well as other possibilities with different sample rates collection of data.

With this study, the SmartSpark project was concluded. It has often been said that the purpose of this work is to automate the EHDA process. Throughout the practical study, we have tried to concentrate on the basic fundamentals of fluid mechanics and EHDA technology to provide a firm background for proceeding to applications and advanced topics related to it. As you know, we have only covered one set of geometry for the E/HDA in the text and omitted the results from different setup because we could not have more time to do more experiments.

4.1 Recommendations

Power supply, pump and cables connections will fail and must check regularly. Oscilloscopes use high voltages to amplify signals so that they can be displayed on a screen. However, this amplification process can also amplify noise, resulting in a signal that is full of static and other interference. This noise can make it difficult to interpret the signal, and in some cases, can even cause the oscilloscope to malfunction.

Besides that, some fluid leak was causing sparks and consequently wrong measurements. It is very important to keep the setup and the working place clean. This can be done via: 1) removing unnecessary objects; 2) always verify the setup before starting; 3) ask a colleague to double check the setup again; 4) go through safety procedures.

The power supply's internal voltage and current measurements can be polled via an USB interface and could not be included in the data logging because the output is for DC, and the SmartSpark has AC current. All the output from the power supply related to the current was wrong.

4.2 Proposals for Continuing, Limitations and Improvements

For future research, a few things must be taken into account. Starting with the measuring of the properties of the solutions that are used during the ES concept. Therefore, it is advised to continue with testing liquid properties before ES measurements. Knowing the correct properties, including

conductivity, viscosity, and surface tension, can lead to the repeatability of the experiments and the necessary starting point for electrospraying.

There is always room for improvement in terms of setup, welding, liquid checks, repeatability and repeatability of the procedures performed. Time is a crucial variable and because of that this project can be more explored in the future.

In relation to improve the identification of the spray-mode, an option would be the application of neural networks for classification. The JSON data sets can further be used to train a neural network for an alternative classification approach. The stored data is also used to confirm existing relationships between quantities like e.g. current, fluid conductivity, flow rate, etc. In relation to the SC or TS, probability functions to represent information and drawing inferences from it (deduction) and dealing with uncertain events (sparks) can be done.

Moreover, it is recommended to continue the closed loop system that has been implemented. It is where the output of the system goes to the feedback to the input of the system. This feedback can be used to stabilize the system. The feedback can be used to make the system more stable by making the system more responsive to changes in the input. The feedback can also be used to make the system less stable by making the system less responsive to changes in the input.

There is a region of the cone-jet and stable multi-jet that allows us to use the theory behind the Control Systems, which can help to discover the region that we have the most stable mode. In order to do this, we get the voltage value from the power supply as the feedback value and we have the closed loop system. More tests need to be done with different liquid in order to see if the code can be applied in every condition.

Fortunately, many modern design tools—both professional and student versions are available, as well as open source software modules and Internet-based user groups (to share ideas and answer questions), to assist the controller modeler. The implementation of the control systems themselves is also becoming more automated, again assisted by many resources readily available on the Internet coupled with access to relatively inexpensive computers, sensors, and actuators.

Unwanted random interference, or noise, is present to some extent in all communication, measurement, and recording situations. We must be aware of it and know that it imposes a fundamental limit on information carrying capacity. The results must always be concerned about what happens when noise current produces a voltage across the ES system. Because of this, it is a good idea to calculate the noise current modulation waveform for each oscillator noise source using a simulator.

Finally, detecting plasma forming and reducing the voltage over nozzle to counter electrode but also using the liquid conductivity itself to limit the current is also positive, hence introducing a resistance in the few GigaOhm adding a few GigaOhm resistor into the current path could be an improvement.

References

- [1] (2012). Bio-decontamination of water and surfaces by dc discharges in atmospheric air. *Plasma for Bio-Decontamination, Medicine and Food Security, NATO Science for Peace and Security Series A: Chemistry and Biology*, 1(1):107.
- [7cb56569] 7cb56569, I. E. R. Api documentation.
- [3] Akishev, Y., Grushin, M., Kochetov, I., Karalnik, V., Napartovich, A., and Trushkin, N. (2005). Negative corona, glow and spark discharges in ambient air and transitions between them. *Plasma Sources Sci. Technol.*, 1(1):18–25.
- [4] Chen, D.-R., H., D. Y., and L., P. K. S. (1995). Experimental investigation of scaling laws for electrospraying: Dielectric constant effect. *Aerosol Science and Technology*, 1:27:3,367–380.
- [5] Crowley, N. Getting started with python and influxdb.
- [6] Crowley, N. Getting started with python and influxdb.
- [7] de la Mora, J. F. and Loscertales, I. (1994). The current emitted by highly conducting taylor cones. *Journal of Fluid Mechanics*, 1:155–184.
- [8] Doebelein, E. O. (1990). *Measurement Systems - Application and Design*. McGraw-Hill.
- [Durdle] Durdle, H. How (not) to kill your pi's sd card.
- [10] Gañán-Calvo, A. M. (2004). On the general scaling theory for electrospraying. *Journal of Aerosol Science*, 1(1):203–212.
- [11] Gañán-Calvo, A. M., J.C.Lasheras, Davila, J., and Barrero, A. (1997). Current and droplet size in the electrospraying of liquids, scalin laws. *Journal of Aerosol Science*, pages 249–275.
- [12] Gañán-Calvo, A. M., Rebollo-Muñoz, N., and Montanero, J. M. (2013). The minimum or natural rate of flow and droplet size ejected by taylor cone?jets: physical symmetries and scaling laws. . *Phys. Rev. 10*, 1(1):1–6.
- [IBM] IBM. What is ppp.
- [14] Joan, R.-L., Jordi, G., and G., L. I. (2018). Electrosprays in the cone-jet mode: from taylor cone formation to spray development. *Journal of Aerosol Science*, 1(1).
- [15] Labs, G. (2022). Dashboard json model.
- [16] Lynn, P. A. and Fuerst, W. (1999). *Introductory Digital Signal Processing with Computer Applications*.

- [17] M., G.-C. A., M., L.-H. J., A., H. M., A., R., and M., M. J. (2018). Review on the physics electrospray: from electrokinetics to the operating conditions of single and coaxial taylor cone-jets, and ac electrospray. *Journal of Aerosol Science*, 1(1):203–212.
- [18] M., P., R., B., and Albanese (2013). The global prevalence of dementia: A systematic review and metaanalysis. *Alzheimers & Dementia*, 9(1):63–75.
- [19] M. Cloupeau, B. P.-F. (1994). Electrohydrodynamic spraying functioning modes: a critical review. (1):63–75.
- [20] Muñoz, A. J. C. (2021). *Production of Homogeneous Particles by Controlled Neutralization of Electrosprays*.
- [Nair] Nair, A. Introduction to influxdb: A time-series database.
- [ngrok community] ngrok community. Getting started with ngrok.
- [23] Pai, D. Z., Lacoste, D. A., and Laux, C. (2010). Transitions between corona, glow, and spark regimes of nanosecond repetitively pulsed discharges in air at atmospheric pressure. *Journal of Applied Physics*, 1(1):107.
- [24] Profa. Carmela Maria Polito Braga, Prof. Hugo César Coelho Michel, D. (2021). Aula 01: Programação de sistemas de controle utilizando o padrão iec 61131-3; linguagens: Blocos funcionais e diagrama ladder. *DELT/UFMG*, 1:43.
- [25] Singh, A. (2021). *Mobile Computing*.
- [26] Taylor, G. I. (1964). Disintegration of water drops in a electric field. *Proc. R. Soc. Lond.*, 1(1):280–397.
- [27] Verdoold, S. (2012). *Electrohydrodynamic atomisation—unipolar and bipolar characterisation and modelling (Ph.D. thesis)*. Delft University of Technology,.
- [28] Verdoold, S., Agostinho, L., Yurteri, C., and Marijnissen, J. (2014). A generic electrospray classification. *Journal of Aerosol Science*, pages 505–517.
- [WaveShare] WaveShare. Sim7600x 4g hat guides for pi.
- [30] Zeleny, J. (1917a). Electrostatic spraying of liquids in cone-jets mode. *J. Electrostatics*, 1(1):135–159.
- [31] Zeleny, J. (1917b). Instability of electrified liquid surfaces. . *Phys. Rev. 10*, 1(1):1–6.

5 Appendices

In order to reproduce the experiments again, we need a pattern in the measurements. High speed camera requires more light and distance affects the system. Despite that, the liquid properties were collected at WETSUS: European Centre of Excellence for Sustainable Water Technology and the details of the instruments can be seen in the Appendices (see Figure 51 ?? 50 ??).

The company that made the nozzle from the setup was Venema Fijnmechaniek B.V. (see figure ??). All nozzles were made of conducting materials inside.

Final Control Elements are those responsible for manipulating the flow of matter and/or energy, aiming to act on the process in order to correct the value of the controlled variable whenever there is some deviation from the reference. The most commonly used final control elements are control valves, in different models, materials and dimensions, according to the application. We had to use valves in order to build the co-flow system in the setup. See the correct manner to build it in Figure 52.

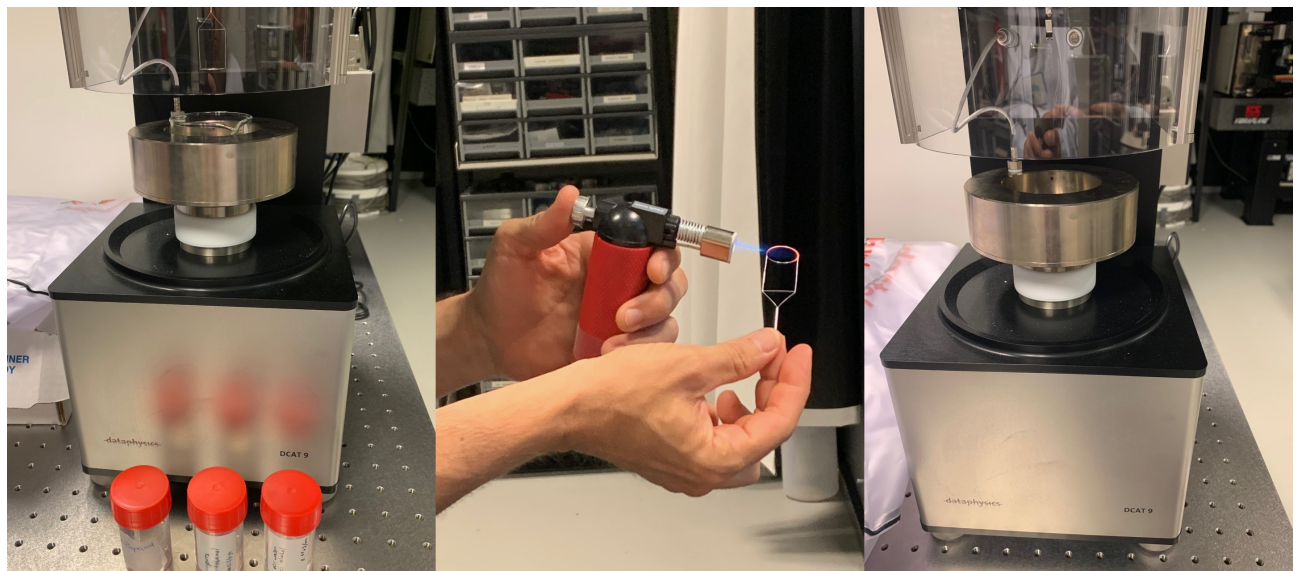


Figure 50. Surface tension measurement DCAT – Dynamic Contact Angle measuring devices and Tensiometer, Ring and plate tensiometer DCAT 9, by DataPhysics Instruments at WETSUS

Acknowledgements

This work was supported by the Water Technology Application Center, at Van Hall Larenstein (VHL), University of Applied Sciences (VHL), in Leeuwarden, The Netherlands. It was supported by Regieorgaan SIA, TiePie Engineering and YNOVIO B.V.. This project was linked to NHL Stenden University. NHL Stenden is a leading EHDA group in The Netherlands. The university is cooperating with Van Hall Larenstein University of Applied Sciences and Wetsus in this area which resulted in the Gilbert-Armstrong Lab for Electrohydrodynamics. An unique environment in the Netherlands

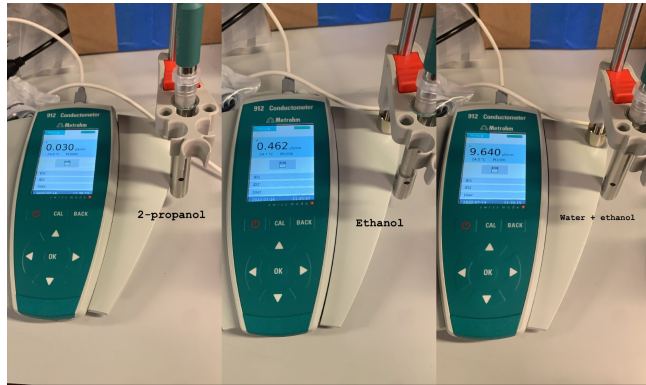


Figure 51. Electrical conductivity measurement approach at Van Hal Larenstein with 912 Conductometer from Metrohm



Figure 52. Valve's order for connections in the setup (*Valves*)

for the conduction of EHDA related research. TiePie Engineering is a Dutch SME specialized in the development of compact measurement equipment and measurement data logging devices located in the city of Sneek. For this project, the company offers expertise in measurement setups with high sampling rates (up to 1GSamples/s) and some digital signal processing functions. They also have profound expertise in circuit board design for high frequencies (rise times of low energy partial discharges are equivalent to frequencies ranging between 500 MHz to 1 GHz). Ynovio B.V. is an on-demand electronics solutions company. Together with TiePie, both companies could provide the necessary electronics input as well as are seen as technological providers. TiePie also has the expertise to further develop the project outcome towards an industrial product. I would like to thank the whole team for supporting this research project.